Design and Optimization of Porous Polymer Enzymatic Digestors for Proteomics

Wei Lin

A Thesis

in

The Department

of

Chemistry and Biochemistry

Presented in Partial Fulfillment of the Requirements
for the Degree of Master of Science (Chemistry) at
Concordia University
Montreal, Quebec, Canada

July 2009

Your file Votre référence
ISBN: 978-0-494-63071-6
Our file Notre référence
ISBN: 978-0-494-63071-6

CONCORDIA UNIVERSITY

School of Graduate Studies

This is to certify that the thesis prepared

By: Wei Lin

Entitled: Design and Optimization of Porous Polymer Enzymatic Digestors for Proteomics

and submitted in partial fulfillment of the requirements for the degree of

Master of Science (Chemistry)

complies with the regulations of the University and meets the accepted standards with respect to originality and quality.

Signed by the final examining committee:

_____ Chair

_____ Examiner

_____ Examiner

_____ Supervisor

Approved by _____

Chair of Department or Graduate Program Director

_____ 20__ _____

Dean of Faculty

Abstract

Design and Optimization of Porous Polymer Enzymatic Digestors for Proteomics

Wei Lin

Effective protein characterization and identification is a demanding and time-consuming operation in proteomics because of long protein purification/separation procedures and even longer enzymatic digestions. In this work, polymer-based monolithic enzyme reactors were fabricated in fused-silica capillaries, and performance was characterized through protein digestion and identification by MALDI-MS and ESI-MS. Trypsin and *Staphylococcus aureus* V-8 protease (Glu-C) were used to produce three types of reactors: trypsin-based, Glu-C based and tandem trypsin Glu-C. Reactors were prepared by synthesizing a porous methacrylate base monolith followed by photografting with glycidyl methacrylate, and immobilization of the enzyme(s) with carbonyldiimidazole. Protein digestions, performed by perfusing protein solutions through the reactor under pressure, were evaluated based on the peptide map generated when directly coupled to an ESI mass spectrometer. Excellent digestion efficiencies were observed over a flow rate range from 0.2 to 1 $\mu L\ min^{-1}$, which corresponds to reactor residence times of 1.4 to 0.24 min. As a proof of principle application of a complete proteomics analysis, chromatographic separation of model proteins followed by digestion of specific fractions using these proteolytic enzyme reactors and ESI-MS is demonstrated.

Acknowledgments

I would like to express my sincere gratitude to Dr. Cameron Skinner for his full support, inspiration, and encouragement during my research work. I would also like to thank my committee members, Dr. Ann English and Dr. Joanne Turnbull, for their sparking advice and guiding. Many thanks to my colleagues and friends who helped me fulfill this task, especially to: Jean-Louis Cabral, Michel Boisvert, Vincent Lau, Alexander Lawandi, Maria Kaltcheva, Lynn Miller, Alain Tessier (CBAMS, Concordia University) for his help in MS analysis, Yan Hao Tao (Concordia University) for BET experiments, and Raymond Mineau (Université du Québec à Montréal) for SEM acquisition. Last but not least, I would like to acknowledge my beloved life partner, Jee In Song, who is always there to share my success and failure.

Table of Contents

List of Figures

List of Tables

List of Abbreviations

ACN	Acetonitrile
ACTH	Adrenocorticotropic hormone fragment 1-10 human
AMPS	2-Acrylamido-2-methyl-1-propanesulfonic acid
BAC	Butyl acrylate
BDDA	1,3-Butanediol diacrylate
BET	Brunauer-Emmett-Teller
BME	Benzoin methyl ether
BSA	Bovine serum albumin
CE	Capillary electrophoresis
CID	1,1'-Carbonyldiimidazole
ESI-MS	Electrospray ionization mass spectrometry
Glu-C	*Staphylococcus aureus* V-8 protease
GMA	Glycidyl methacrylate
HPLC	High performance liquid chromatography
ID	Inner diameter
MALDI-MS	Matrix-assisted laser desorption/ionization mass spectrometry
MS	Mass spectrometry
OD	Outer diameter
PEG	Poly (ethylene oxide)
SEM	Scanning electron microscope

Chapter 1 Introduction

1.1 From genomics to proteomics

The ultimate goals of the life sciences are to determine the functions of genes and their products, to further understand how they are linked into biochemical pathways and/or networks, and to eventually develop a fuller understanding of how biological systems work [1]. Dramatic advances in the life sciences began in the 1990's as large-scale DNA sequencing became possible due to technological breakthroughs and ushered in the genomics era in which masses of sequence data were generated (Figure 1-1). The genome is defined as "a complete single set of the genetic material of a cell or of an organism; the complete set of genes in a gamete." [2]. In 1995, the first complete cellular genome sequence (*Haemophilus influenzae*) was published. In the subsequent years, more than 100 genome sequences were completed, including the human genome in 2003 [1]. On April 15, 2009, GenBank reported that more than 102 billion base pairs in over 103 million sequences have been released, and stated that "From 1982 to the present, the number of bases in GenBank has doubled approximately every 18 months".

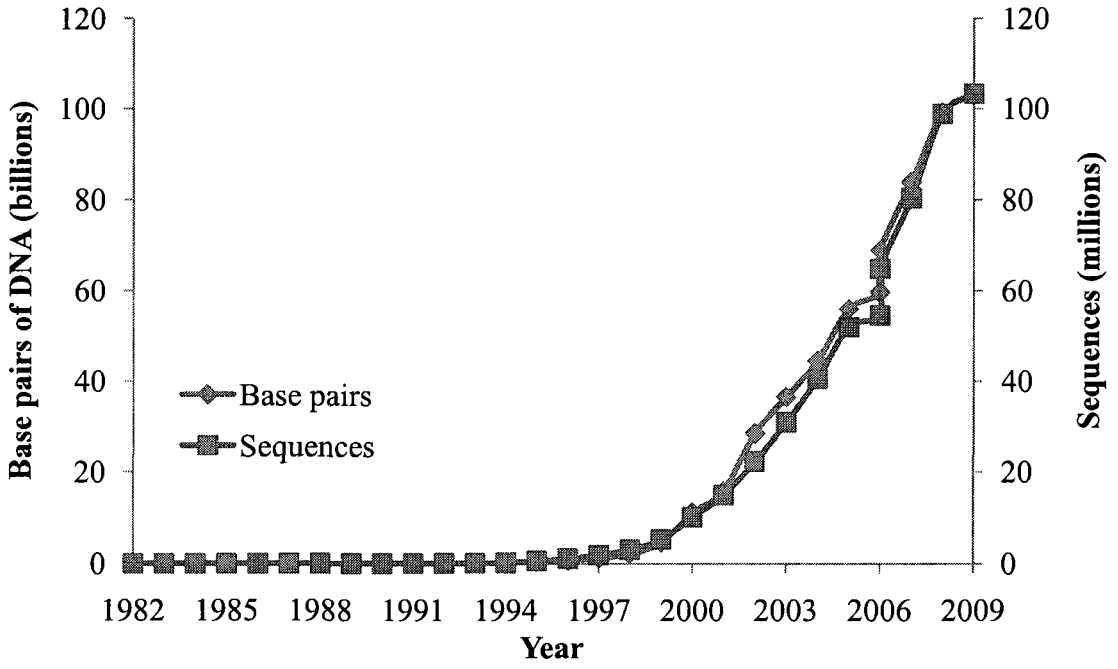

Figure 1-1: Growth of the GenBank database. Data obtained from the GenBank release notes (April 15, 2009).

Even though much knowledge has been gained from genomics, the workings of biological systems still remain as an unresolved challenge. Nucleic acids, the major focus in genomics, are only information carriers, indirectly and sometimes insufficiently providing information about protein function. Proteins are the actual functional molecules in biological systems, participating in all the biochemical activity of the cell by interacting with one another and with a large variety of other molecules. Therefore, the direct study of proteins, *i.e.* proteomics, has received remarkable attention due to its critical role in advancing knowledge for the Life Sciences, the identification of disease processes, and in understanding drug actions [3, 4].

The term proteome was coined by Humphrey-Smith *et al.* [5] in 1995, as "the total protein content of a genome". By a broader definition, proteomics involves the study of complex mixtures of proteins and their interactions [6]. In contrast to the

genome, the proteome is highly dynamic since the type of proteins expressed, their abundance, extent of modification, at any given time and location, are dependent on the physiological state of the organism or signals from the environment. The proteome is much more complex than the genome since a single gene can generate many different proteins by alternative use of start and stop codons and by various modifications during and/or after translation. Due to the complexity of proteomics, a range of different technological approaches have been utilized for a variety of analysis, such as affinity purification, biochemical assays, microarray, chromatography, and mass spectrometry. The current challenge is complete integration and automation of these technologies, an important factor that enhances the success of genomics. In addition, sensitivity is another issue that needs to be improved. Since an amplification method (PCR for DNA sequencing) for scarce proteins is not available, analysis of the lowest abundance proteins is always difficult. Therefore, new or better materials, instrument design and methodologies are required to facilitate proteomics by providing a comprehensive analysis of complex biological systems.

1.2 Enzymatic digestion in proteomics

In general, there are two approaches used in proteomic surveys, top-down and bottom-up. The top-down approach commences with the separation of a complex mixture of proteins, harvested from the system under study followed by proteolytic digestion of specific fractions and identification of the components in those fractions based on the peptides generated [7]. On the other hand, bottom-up proteomics relies on peptide mapping, in which all the proteins in the sample are digested first, followed by separation of the peptides and identification of these peptides [8]. Both techniques

usually rely on mass spectrometry for peptide identification. No matter which proteomic approach is employed, separation, enzymatic digestion, and peptide identification are required.

For each step in the proteomic sequence, there are several techniques available to choose from. For example, high performance liquid chromatography (HPLC) or capillary electrophoresis (CE) are commonly used for the separation whereas mass spectrometry (MS) or Edman sequencing are available for peptide identification. Only the enzymatic digestion was limited to one technique until the method of enzyme immobilization was introduced. Conventionally, enzymatic digestion is achieved by incubation of the protein(s) and protease in a suitable buffer solution from 22 to 37 ^{o}C [9, 10]. To minimize proteolytic autolysis which diminishes activity of proteases and complicates data analysis due to the presence of autolysis peptides that may cause false identification of the target protein using data base searching, low protease to substrate ratios are used, typically 1:20-1:100 w/w that necessitate extended incubation times of 3-24 hours that lower the digestion efficiency. An additional limitation of in-solution digestion is that it often includes extensive manual sample handling steps.

The new concept of using immobilized proteases in microreactors for protein digestion has drawn significant attention during the last few decades [11-14]. In these microreactors (capillaries or microfluidic chips), proteases are attached to the surface of the channels or stationary phase. Proteins are digested by the immobilized proteases when they move with the mobile phase into the digestion zone, forming peptides that are swept out of the digestion zone and can be detected either off-line or on-line. This method has a number of advantages over the in-solution digestion method, such as

minimization, or even elimination, of protease autolysis, larger enzyme to substrate ratios, shortened digestion time, and high digestion efficiency [12]. More importantly, these microreactors can be easily coupled with mass spectrometers to perform automated on-line protein characterization [11], which is a step forward in the development of an integrated and automated analytical system for proteomics.

1.3 Enzyme immobilization techniques

A variety of proteases, such as trypsin [15-19], chymotrypsin [20], pepsin [21, 22], elastase [23], and papain [24], have been immobilized onto both the walls and support packings in capillaries and microfluidic chips. In the literature, enzymes were attached to the support primarily through three methods, covalent binding [25], physical adsorption [26-29], and sol-gel encapsulation [30, 31].

The main advantage of covalent attachment is the minimization of leakage of proteases from the reactors. There are several potential sites on proteases that can be used for attachment, including amino groups on the backbone chain or on lysine and arginine residues; carboxyl groups on the backbone chain or on aspartic and glutamic acids; the phenol ring of tyrosine; the thiol group of cysteine; the hydroxyl groups of serine and threonine; the imidazole group of histidine; and the indole group of tryptophan [14]. To prevent modification or inactivation of the proteases, the potential binding site for immobilization needs to be cautiously investigated. It is important that the catalytic groups of the protease and the functional groups located in the active site are not involved in covalent linkage to the support. Furthermore, the active site of the protease might not be accessible after immobilization due to steric hindrance in which the active site is not exposed to substrates. This problem can be minimized by introducing a spacer molecule

which distances the protease from the surface of the support and conveys flexibility onto the enzyme molecule [32].

Physical adsorption may be the simplest means for enzyme immobilization. The enzyme and surface of the support are bound by a variety of forces, such as ionic interactions, hydrogen bonds, van de Waals forces, and hydrophobic interactions. Besides these interactions, bio-specific adsorption is another choice which has shown some success. A good example is the biotin-avidin/streptavidin adsorption [33, 34], which offers oriented immobilization, resulting in relatively good accessibility to the active site center. The strength of the binding between biotin and avidin is very strong ($K_d = 10^{-15}$M [34]), so this type of reactor can tolerate extreme conditions of temperature and pH. Compared to covalent binding, physical adsorption requires fewer reaction steps and results in less change of enzymatic activity. However, the stability of the immobilized enzymes is much lower, resulting in enzyme leakage and shorter reactor lifetime.

The sol-gel encapsulation method enables incorporation of enzymes into a gel matrix fabricated by hydrolysis of a suitable precursor followed by condensation to yield a wide range of linear, bridged polymeric networks [30]. During the polymerization and gelation process, the enzymes that are mixed with the precursor are trapped in the matrix. By necessity, the reaction takes place under mild conditions, so the enzyme can maintain its structure and activity. In recent years, several sol-gel techniques to modify polymer microfluidic chips for trypsin immobilization have been developed, including silica, alumina, and titania [35, 36]. The main drawback of the reactors prepared by sol-gel

encapsulation is that the digestion is slow because the rate of mass transfer of both substrate and product relies on diffusion into and out of the sol-gel matrix [11].

1.4 Organic monoliths: popular support for enzyme immobilization

Monoliths are defined as a single piece of highly porous material [37]. A monolith can also be described as a single large "particle" without interparticulate voids that typically exist in traditional packed columns. The pores inside the monolith are open, consisting of a highly interconnected network of channels. During the late 1960's and the early 1970's, attempts to develop the "single-piece" stationary phases for LC separations were not successful. Interest in monolithic separation media then faded for almost two decades until the modern monoliths were introduced as HPLC stationary phases in 1989 [38]. Hjertén *et al* designed a column filled with cross-linked polyacrylamide gel, demonstrating an excellent chromatographic separation of proteins in ion-exchange mode. Soon thereafter, this type of monolithic columns became commercially available from BioRad Laboratories (Figure 1-2). Monolithic stationary phases were further developed by František Švec and Jean Fréchet at the University of California at Berkeley in the 1990's, introducing monolithic flat discs [39] and monolithic capillary columns [40] for nano-HPLC and electrochromatography using new methods for fabrication and modification, such as photo-initiated polymerization and grafting. These micro-monoliths were then applied not only for separation of bio-molecules, but also as enzyme reactors.

A)

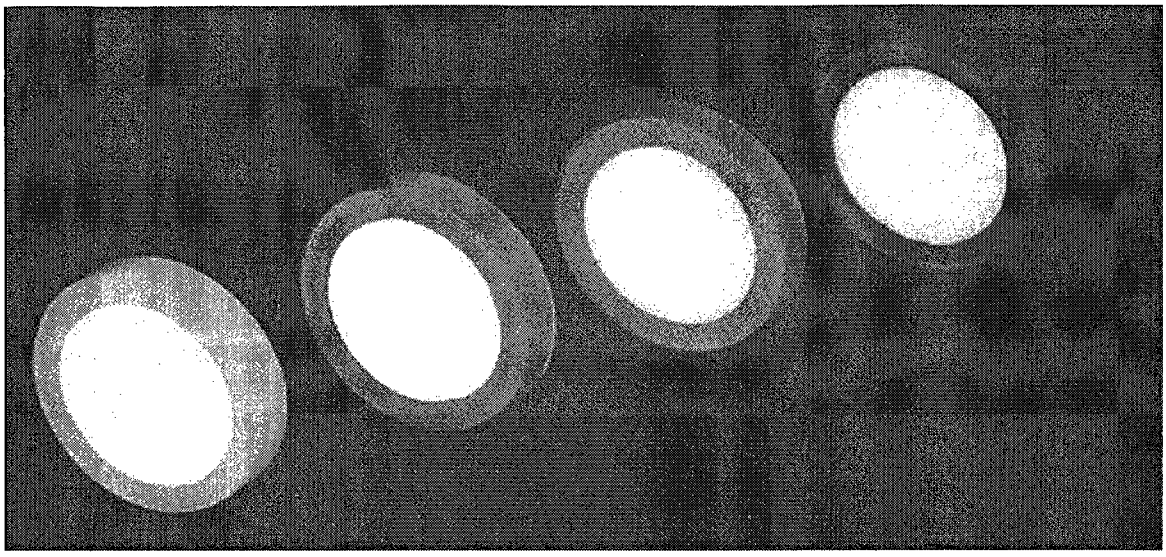

B)

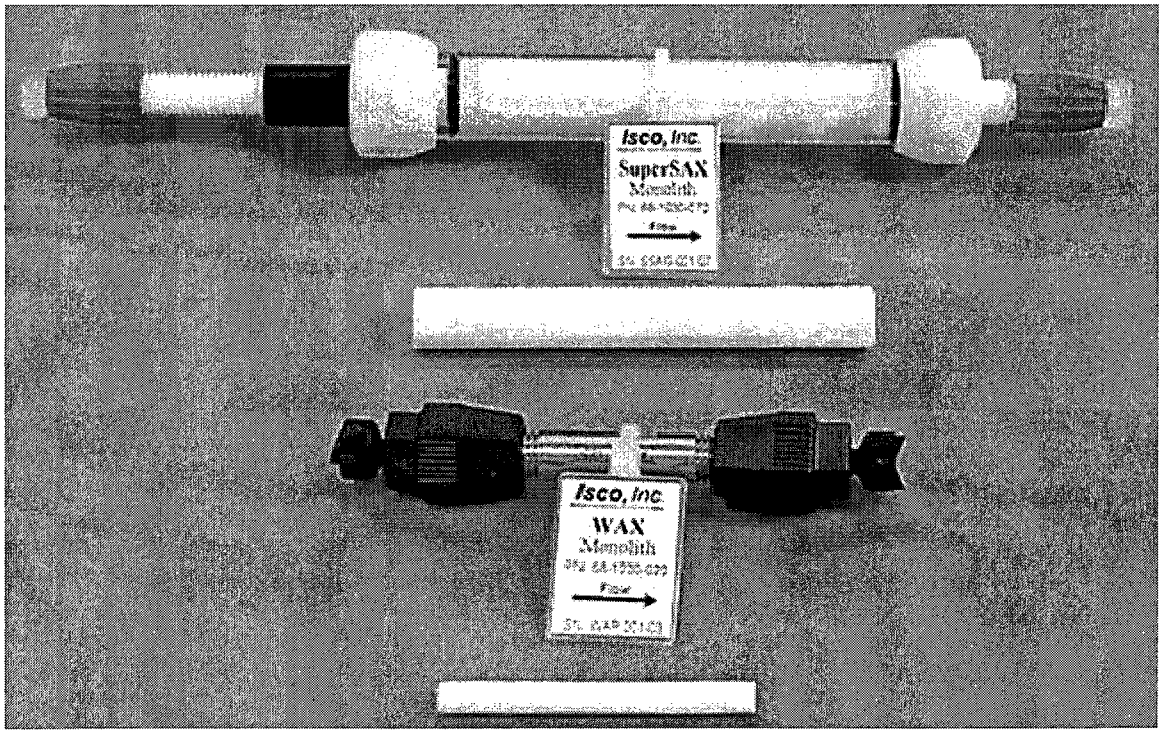

Figure 1-2: Commercial monolithic columns in the disk and tube format. A) CIM® Disk monolithic columns. The color of the ring indicates specific chemistry of the disc; B) Glass (upper column) and stainless steel (lower column) Swift® monolithic columns and the corresponding monoliths. (adapted from [41])

Generally, the monolithic support that anchors the proteases in micro-reactors can be divided into two groups, silica-based [42-44] and organic polymer-based [45-51]. Scanning electron microscope (SEM) images of silica and organic polymer-based monoliths are shown in Figure 1-3. Silica-based supports (either the capillary wall or a sol-gel monolith) are not utilized as extensively as their organic counterparts mainly because of the limited chemistries available for silica, potential non-specific interactions with silanol groups, and low stability at extreme pH conditions. On the other hand, organic monoliths are popular as the support for immobilized enzymes [11]. The key reasons seem to be the absence of interparticulate voids, fast mass transfer kinetics, ease of fabrication and facile modification with a wide variety of chemistries [37, 52].

A)

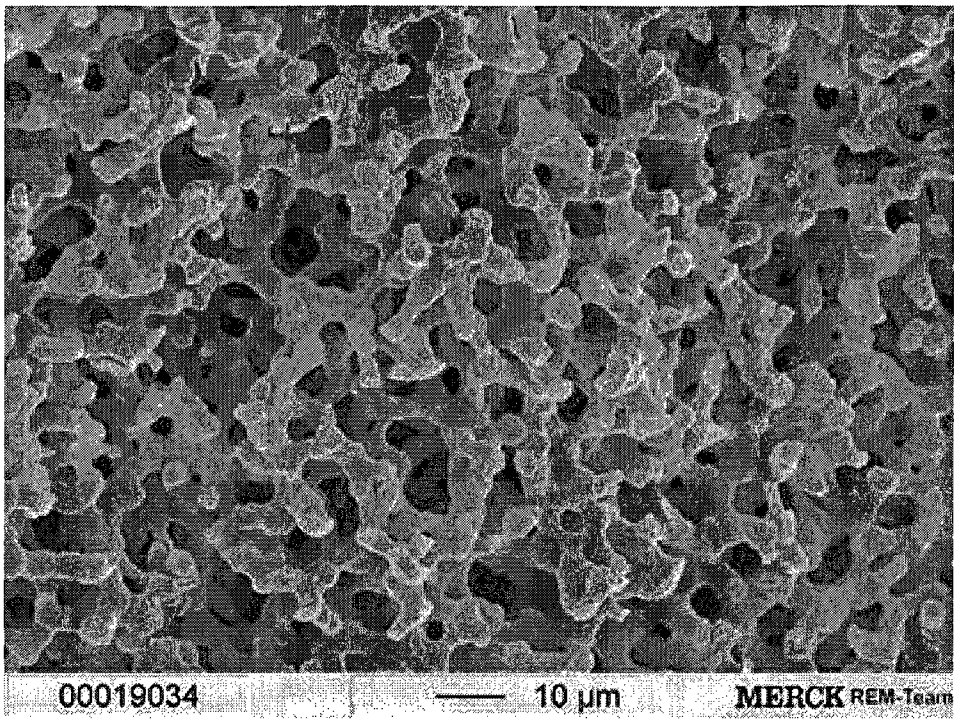

B)

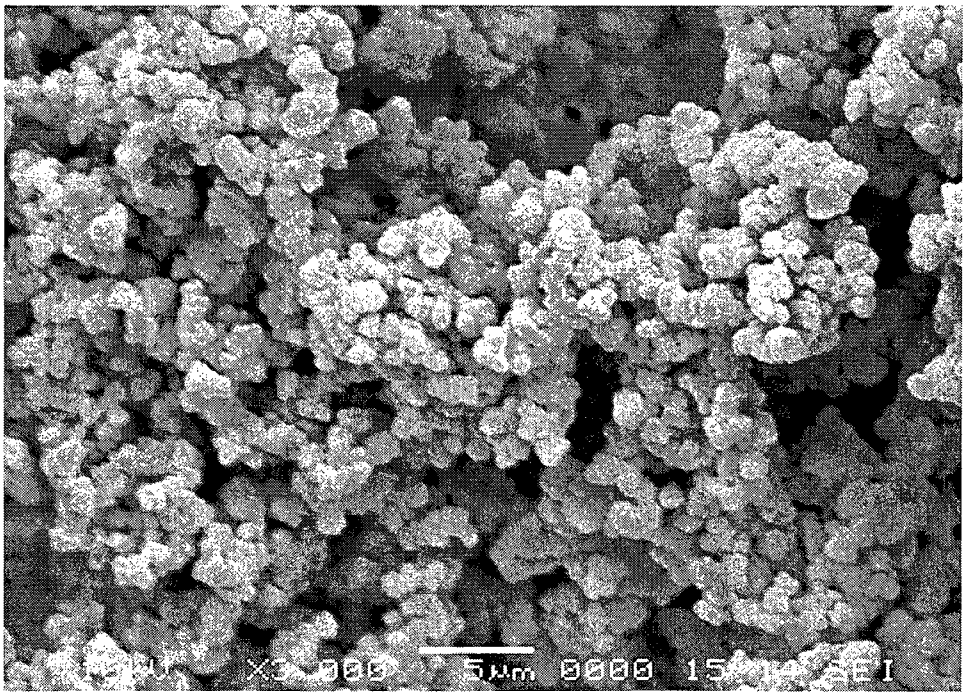

Figure 1-3: SEM images of monoliths. A): silica-based monolith [53]; B): organic polymer-based monolith [37].

The partition of molecules between the mobile phase and the pores of a standard macroporous material (*e.g.*, that found in HPLC columns) is controlled by diffusion.

Generally, due to their much larger diffusion coefficients, small molecules move relatively quickly, whereas large molecules travel between the two phases slowly. The slow mass transfer limits the overall rate of partition, and is deleterious in both chromatography and catalysis.

In a traditional column packed with macroporous particles, the mobile phase primarily flows through the interstitial voids between the particles because of the low resistance it encounters. However, the majority of the stationary phase surface area is found within the pores. The mobile phase within these pores is stagnant, so the only mechanism to transport molecules into and out of the pores is diffusion. The driving force for the diffusion is the concentration gradient created as the analyte plug passes through the column [54]. Relying on diffusion for mass transport is not problematical for small molecules, since they have high diffusion rates and consequently fast mass transfer kinetics. However, for large molecules, for instance proteins digested in a traditional packed column with immobilized proteases, the situation is quite different. Proteins diffuse slowly through the mobile phase into the pores where much of the proteases is located. Once there, and cleaved by the active site, the products must also diffuse back to the moving mobile phase. If diffusion is the rate determining step, only those proteases located in close proximity to the particle exterior surface are readily accessible by the proteins. Consequently, the efficiency of the protease reactor will not reach its full potential [55].

Contrarily, using monolithic stationary phases can dramatically improve the access to the functional groups in the stationary phase, and ultimately increase the mass transfer kinetics. Since there are no interparticulate voids, the mobile phase flows

through the monolith. This convective flow brings the protein to the surface and removes the products rapidly which significantly accelerates the mass transfer. As a result, much higher efficiencies can be obtained from monolithic columns both in chromatographic separations [56] and biocatalysis [57].

There are three types of organic polymer monoliths used in enzyme reactors, acrylamide copolymers, methacrylate copolymers, and vinylazlactone copolymers. Among them, methacrylate copolymers are the most widely investigated and understood. The methacrylate monoliths are usually fabricated via a copolymerization reaction of an initiator, a functional monomer and a crosslinking monomer in the presence of a porogenic solvent. The structural rigidity of the monolith is achieved through extensive cross-linking, and the interconnected pores of different sizes in the monolith are obtained due to the presence of the inert porogenic solvent during the polymerization process.

Initiation of the polymerization reaction is commonly achieved thermally, photolytically (UV), or by γ-radiation. In thermally initiated polymerization, a mold containing the reaction mixture is placed in a temperature controlled device, *e.g.*, a water bath. With this method, the solvent system must be chosen carefully. Volatile solvents, such as ethanol, ACN and chloroform, should be avoided because they readily evaporate, leading to uncontrolled pore size. In the UV initiated method, the reaction takes place at room temperature, and generally takes less time and can be limited to the specific location exposed to the UV radiation compared to the thermal method. The last method, γ-radiation initiated reaction, is the least common where the monoliths are prepared using ionizing radiation. The main advantages of this method are direct generation of radicals

from the monomers without any initiator, and the free radicals are homogeneous, resulting in a crosslinked product [52].

The methacrylate-based polymerization reaction takes place by a five-step mechanism [52]. First, the polymerization reaction is initiated by decomposition of the initiator which reacts with the monomers to start the polymer chains. Second, the polymer chains grow, but their low solubility in the porogenic solvent causes them to precipitate to form nuclei. This is followed by the third step, in which the precipitated nuclei accumulate and swell with monomers adsorbed from the solvent in which they have limited solubility compared to the porogenic solvent. Fourth, polymerization in the nuclei occurs as it is kinetically preferred due to the elevated monomer concentration. As the polymerization reaction progresses, the size of the nuclei increase, becoming microglobules and then aggregating to form clusters. Last, the overall morphology is formed as the microglobules continue to grow and crosslink to one another. The final product is a two-phase system consisting of a continuous solid monolith and the liquid porogenic solvent filling the pores.

The functional monomer determines the polarity of the final monolith, whereas the crosslinker and the porogenic solvent affect the size and the distribution of the pores. The porogenic solvents, a mixture of "good" and "poor" monomer solvents, affects the solvation of the polymer chains during early stages of the polymerization, larger pores are generally obtained as a result if poor solvents are used. In addition, the experimental conditions of the monolith fabrication process also have a significant effect on the morphology of the monolith, for example, the irradiation time (UV initiated), lamp power (UV initiated), and temperature [58, 59].

1.5 Facile modification of monoliths

Application of monoliths as either chromatographic stationary phases or supports for immobilized enzymes depends directly on their surface chemistry. The simplest way to obtain the desired surface chemistry is via the copolymerization reaction and using a monomer containing the desired functional groups. For instance, alkyl-substituted monoliths for reverse phase separations were prepared by copolymerization of ethylene dimethacrylate and a hydrophobic monomer, such as butyl methacrylate, and octyl methacrylate [60, 61]. Even though this approach to obtain the desired surface chemistry is simple, it requires re-optimization of the polymerization conditions for each type of polymer which can be a fairly long and complicated process. The porous structure and morphology of the monolith are significantly altered when different monomers or crosslinkers are used.

Glycidyl methacrylate (GMA) is one of the most widely used functional monomers. By taking advantage of the very reactive epoxy groups of GMA, direct surface modifications can be achieved [62-64]. The simplest route to immobilization of enzymes onto GMA-based monoliths is a direct, single-step reaction between the epoxide groups and the nucleophilic groups of the enzymes, such as amino groups on the backbone chain or on lysine and arginine residues, and the indole group of tryptophan. Deoxyribonuclease [65], acetylcholinesterase [66], and trypsin [67] were immobilized using this method. This approach is a simple one step reaction, but the reaction rate is fairly slow, resulting in more than 10 h reaction time. To avoid the disadvantage of the direct reaction on epoxide functionalities, three alternative methods have also been developed. The first approach commences with hydrolysis of the epoxide ring to a diol

and oxidation of the diol to a ketone using periodate, followed by formation of an imine C=N double bond between the monolith and the enzyme. Since the imine double bond is not very stable, hydrogenation with sodium cyanoborohydride is used to convert the imine bond to a stable secondary amine C-NH bond. In another approach, aminolysis of the epoxide ring using ammonia is used instead of hydrolysis, followed by activation with a dialdehyde, most often glutaraldehyde, and the same two reactions with an enzyme described above to complete the immobilization [68]. These two approaches require less time for the entire process, but require more steps. The last method, suggested by Hearn *et al.* [19], includes hydrolysis of the epoxide ring, followed by carbonyldiimidazole (CID) activation and formation of amine C-NH bond between the monolith and the enzyme. Benčina *et al.* [18] immobilized trypsin on monolithic disks and demonstrated that this immobilization reaction is very fast, and can be completed within 1 h. This feature makes this approach a prominent method for immobilization on GMA-based monoliths.

Recently, a new technique, photografting, has been introduced to enable spatial control of surface chemistry within the monolith [69]. In this method, a photomask is used to designate the area of the monolith to be modified, and new functional monomers are photochemically grafted onto the surface of the monolith exposed to radiation. Photografting introduces grafted polymer chains in a high surface density and permits multiple sites with various functionalities at strictly defined locations in the monolith without affecting the pore size or morphology of the monolith. The mechanism of photografting onto a polymer surface using a photo initiator has been elucidated by Rånby [70]. According to Rånby's mechanism, excitation of the photo initiator by UV

light at 200-300 nm causes hydrogen abstraction and formation of free radicals on the monolith surface. These energy-rich radicals then initiate a propagation reaction, resulting in grafting of the new functional monomer to the surface. The counterpart radicals formed simultaneously from the initiator are not able to initiate polymerization in solution due to insufficient energy and are mostly quenched, leading to dimerization or termination of the growing polymer chains. Since the growing polymer chains grafted to the surface also contain hydrogen atoms for abstraction, new chains can grow from them, ultimately forming branched polymer architecture (Figure 1-4).

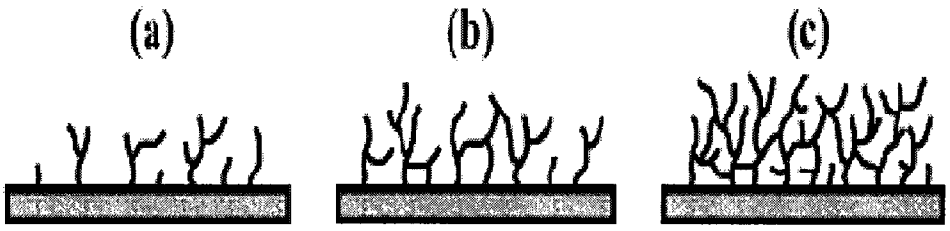

Figure 1-4: Schematic representation of the growing polymer chains with increasing irradiation time. a) Initially, only a limited number of polymer chains grow from the surface. b) The degree of branching increases. C) A dense cross-linked polymer network is formed. (adapted from [71])

The ideal support for enzyme immobilization should have the following characteristics, large hydrophilic surface area; permeability; chemical, mechanical and thermal stability; chemical reactivity for the coupling ligands; and resistance to microbial and enzymatic attack [72]. Organic methacrylate-based monoliths possess all the ideal characteristics except for hydrophilicity. Due to the nature of the functional monomer, the backbone of the methacrylate monolith exhibits significant hydrophobic adsorption of proteins, especially in highly aqueous mobile phases. For proteolytic reactors, the

surface of the monolith must be modified to be more hydrophilic. Poly (ethylene oxide) (PEG) is widely used as a coating material on hydrophobic surfaces to reduce protein adsorption [73, 74]. PEG layers covalently attached to hydrophobic surfaces are believed to prevent protein adsorption by direct coverage of the surface, resulting in blocking of the adsorption sites for proteins [75].

1.6 Proteases utilized in this thesis

Proteases are enzymes that break down proteins by hydrolysis of the peptide bonds of the proteins. They have been used intensively in proteomics, *e.g.* identification of proteins and study of post-transcriptional modification.

In this thesis, trypsin and Glu-C were chosen as good initial candidates for proteolytic enzymes due to their high specificity and popularity in proteomic research. Trypsin (MW 24 kDa) specifically cleaves peptides on the C-terminal side of lysine and arginine amino acid residues, and no cleavage occurs if a proline residue is on the carboxyl side of the cleavage site. Glu-C (MW 29 kDa) hydrolyzes peptide bonds at the carboxyl side of glutamyl and aspartyl amino acid residues. The specificity of Glu-C is dependent on the buffer and pH used. This protease preferentially cleaves glutamyl bonds in ammonium acetate (pH 4.0) or ammonium bicarbonate (pH 7.8), whereas it cleaves both glutamyl and aspartyl amino acid residue sites in phosphate buffer (pH 7.8) [84].

1.7 Thesis objectives

Several research groups have directed their work towards the development of bottom-up, on-line protein characterization systems consisting of a high-throughput proteolytic reactor followed by liquid chromatography or CE separations of the resulting

peptides with MS detection [76-81]. This approach possesses the advantages of automation and sensitivity, but full characterization of the intact protein is not possible. For instance, the molecular weight of the intact protein cannot be determined unless one hundred percent sequence coverage is obtained which is not always achievable. The top-down approach in which on-line digestion is combined with upstream protein separation and downstream peptide detection, on the other hand, has received little attention [82]. This concept was documented by Licklider *et al.* [83], who use immobilized trypsin to on-line digest and identify proteins. However, long digestion times within the digestor (~30 min) were the major obstacle for real-time digestion of proteins as they eluted from the separation step. The top-down approach is worth exploring, since it not only facilitates the association of generated peptides with a particular protein, but it would also aid in the identification of low abundance proteins and *de novo* protein sequencing.

The goals of this thesis are to demonstrate the fabrication of versatile monolithic enzymatic digestors using a photografting immobilization strategy. Once fabricated, this work will show the incorporation of the digestors into an analytical system for top-down automated on-line protein identification.

In order to assess the properties of the base monolithic stationary phase that the enzymes are grafted to, the pore sizes and pore size distribution of the monoliths were characterized by SEM, BET nitrogen adsorption-desorption isotherms, and the total porosity was determined by electrokinetic studies.

Two types of proteolytic reactors, produced by covalently immobilizing trypsin and *Staphylococcus aureus* V-8 protease (Glu-C) onto GMA grafted monolithic supports were then fabricated. Protease activity and specificity were evaluated by quantifying the

immobilized enzymes and by studying the effects of contact time, reactor temperature, and buffer pH on digestion efficiency. Minimization of non-specific adsorption of the proteins/peptides onto the stationary phase was investigated by modification of the surface of trypsin reactors using PEG. Finally, a monolithic column for protein separation and a monolithic tryptic reactor for protein digestion were serially linked for a proof of principle demonstration of top-down automated on-line protein identification.

1.8 Original publications from this thesis

The majority of this thesis has already been accepted for an invited publication in Journal of Separation Science (DOI 10.1002/jssc.200900221). In addition to the results published, more material has been added into this thesis. The additional data is presented in Sections 2.5.2, 2.5.3, 2.6.4, 3.1.2 to 3.1.4, and 3.2.5. Figure 3-17 has also been changed from that presented in the publication as mentioned above.

Chapter 2 Experimental

2.1 Materials and reagents

Unless otherwise stated, all reagents were purchased from Sigma-Aldrich (Oakville, ON, Canada). Glu-C was purchased from Roche (Laval, QC, Canada), and both trypsin and Glu-C were regular biochemical grade. Monofunctional amino terminated PEG was obtained from Polymer Source (Montréal, QC, Canada, MW 5000). The BCA protein quantification kit was from Pierce (Rockford, IL, USA). All solvents were HPLC grade from Fisher (Ottawa, ON, Canada) and mixtures are volume percent unless otherwise noted. Water was obtained from a Barnstead EASYpure® II UV Ultrapure water system (Dubuque, IA, USA) at 18.2 MΩ-cm.

2.2 Preparation of monolithic capillary columns

2.2.1 Column pre-treatment

Fused silica capillaries (UV transparent/Teflon coated 100 μm ID, 365 μm OD or 535 μm ID, 665 μm OD with 5 cm of the polyimide removed) from Polymicro Technologies (Phoenix, AZ, USA) were treated successively with ethanol, 1M sodium hydroxide, and water, followed by a silanization mixture composed of water, glacial acetic acid, and 3-(trimethoxysilyl)propyl methacrylate (50:30:20). After 12 hours, the silanized capillaries were consecutively washed with methanol, water, and then dried with nitrogen gas. The silanization reaction, according to the method described by Ngola *et al.* [85], is shown in Figure 2-1. This pre-treatment functionalized the silica capillaries with a pendant methacrylate group to anchor the polymer wall.

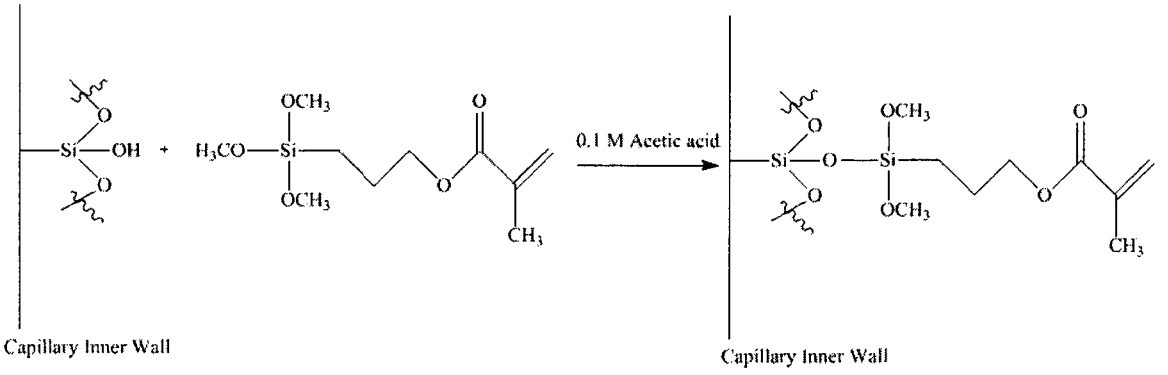

Figure 2-1: Silanization reaction on the capillary inner wall.

2.2.2 Fabrication of monolithic columns

The monomer mixture was composed of butyl acrylate (BAC), 1,3-butanediol diacrylate (BDDA), 3-(trimethoxysilyl)propyl methacrylate (an adhesion promoter), 2-acrylamido-2-methyl-1-propanesulfonic acid (AMPS) (69.2:30:0.3:0.5) and the photo-initiator, benzoin methyl ether (BME, 0.5 wt%), was added just prior to exposure. The porogenic solvent consisted of acetonitrile (ACN), ethanol, and 5 mM phosphate buffer, pH 7.0 (60:20:20). The capillaries were filled with polymerization mixture (1:2 monomer mixture/porogenic solvent) and 10 cm was exposed to UV light for 25 minutes from a high-pressure mercury lamp. Unreacted monomers were purged with ACN at 6.9 bar for one hour. The reaction scheme is summarized in Figure 2-2.

A

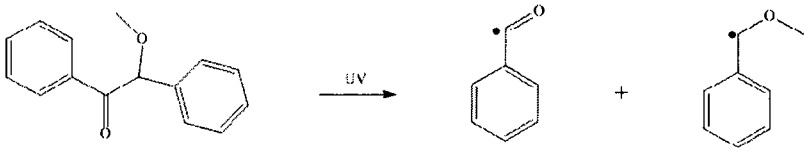

B

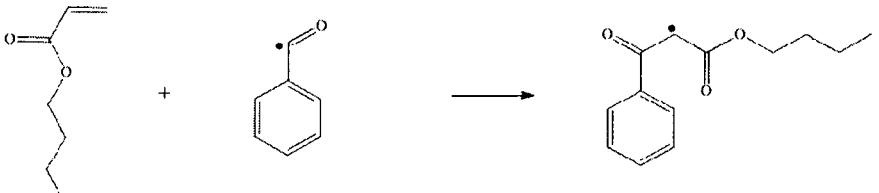

C

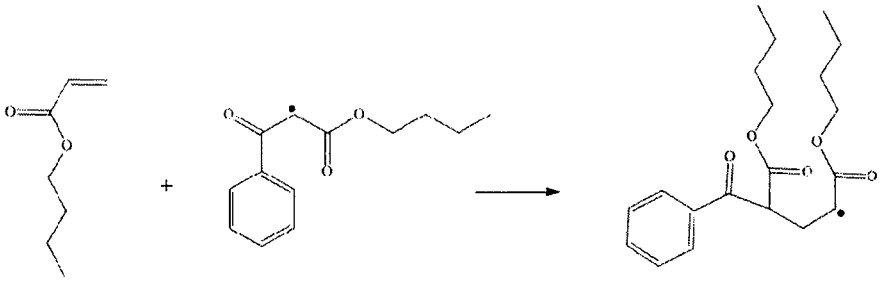

D

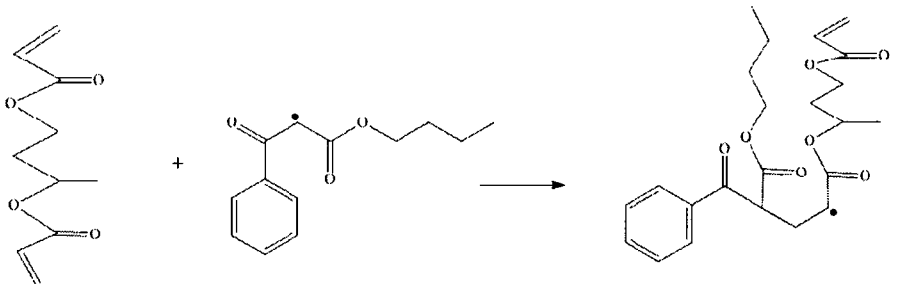

E

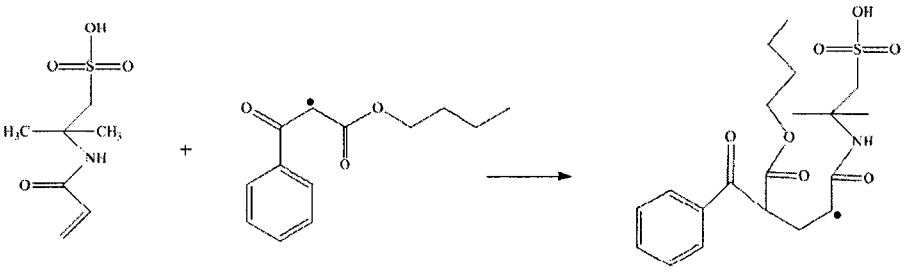

F

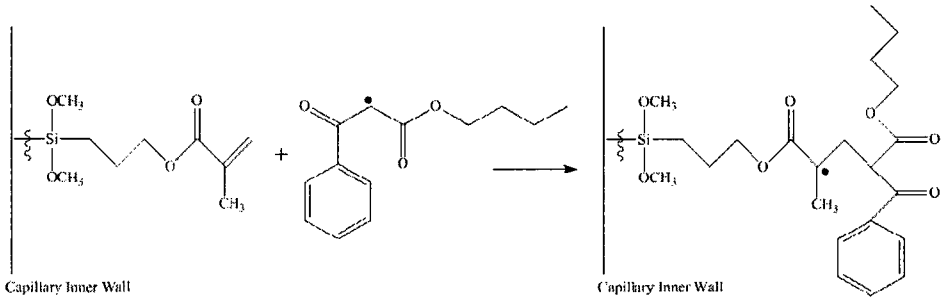

Figure 2-2: Reaction scheme for the synthesis of the base monolith. A) The polymerization is initialized by UV light, producing a benzoyl peroxide free radical; B) the polymer chain then propagates through the reaction between a benzoyl peroxide free radical and BAC; C) the reaction between a BAC radical with another BAC monomeric subunit; D) the reaction between a BAC radical with BDDA; E) the reaction between a BAC radical with AMPS; and F) the reaction between a BAC radical with the silanized capillary inner wall.

2.3 Modification of monolithic capillary columns

2.3.1 Photografting of GMA

The photografting polymerization mixture, 199 μL GMA and 15 mg BME in 1 mL ACN, was flushed through the capillary and the monolith fabricated using the procedure in Sections 2.2.1 and 2.2.2 was exposed to UV light for 10 min. The capillaries were rotated at the 5th minute in the photografting process based on the suggestion from Hilder *et al.* [86]. Unreacted monomers were flushed out with ACN.

2.3.2 Immobilization of proteases

The process for immobilization of trypsin and Glu-C was adapted from the methods of Hearn *et al.* [19] and Benčina [18]. Briefly, GMA grafted monolithic columns were incubated with 0.5 M sulphuric acid overnight at 50 °C and successively rinsed with 90 mM CID, ACN, and 1 mg/mL protease in 0.1 M bicarbonate buffer, pH 8.0, containing 10 mM calcium chloride as an inhibitor using pressure generated flow at 6.9 bar, producing approximately 0.4 μL/min for one hour. The overall immobilization steps are summarized in Figure 2-3. The trypsin-based and Glu-C-based reactors were stored in 10 mM Tris-HCl (pH 8.0), 10 mM calcium chloride and sodium azide (0.02%) at 4 °C prior to use.

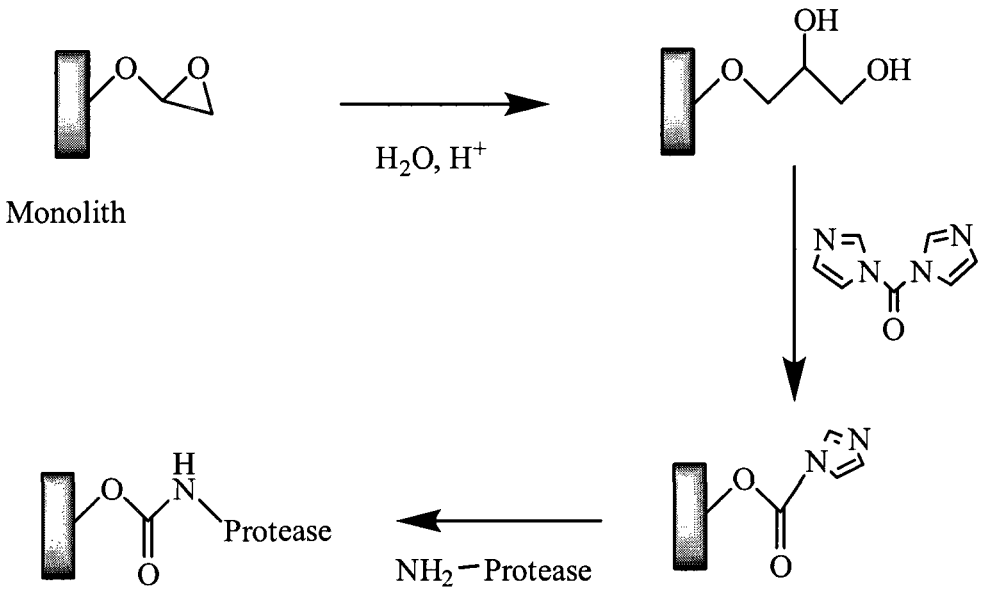

Figure 2-3: Immobilization of protease. Immobilization of proteases was achieved by sequentially photografting GMA onto the monolith, opening the epoxy ring by H_2SO_4, activating with CID, and incubating the desired protease (adapted from [11]).

2.3.3 Immobilization of trypsin and Glu-C in one column

The overall immobilization strategy for immobilizing trypsin and Glu-C in one column is shown in Figure 2-4. Capillary columns containing two 5 cm long sections of monolith (without GMA) separated by 10 cm of open capillary were fabricated as described in Sections 2.2.1and 2.2.2. One section of monolith was GMA modified and trypsin was immobilized on this section by flushing the enzyme through the entire capillary using the same procedure described in Sections 2.3.1 and 2.3.2. Then pressure was applied from the end to be photografted for ½ of the capillary dead time (approximately 100 s) to fill the second section of monolith with GMA grafting solution and exposed to UV for 10 minutes, while the rest the capillary was covered with aluminium foil. Immobilization of Glu-C was carried-out by flushing with 1 mg/mL Glu-

C and 10 mM calcium chloride in 0.1 M bicarbonate buffer, pH 8.0, at 4 °C for two days, and stored using the same procedure described in Section 2.3.2.

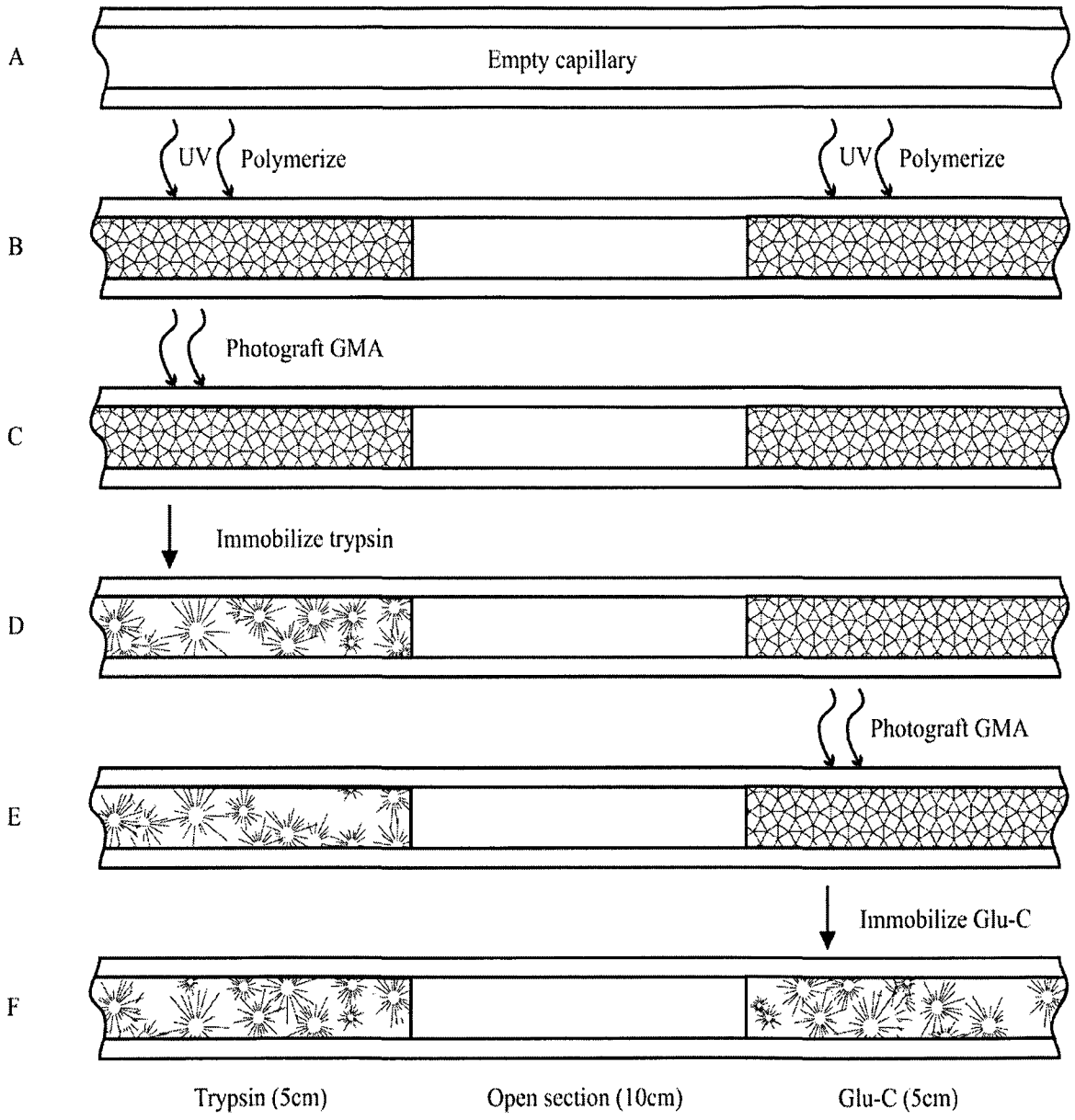

Figure 2-4: Scheme for the preparation of enzyme reactors with two proteases. A) Empty Teflon coated capillary (100 μm ID/365 μm OD); B) monolith column fabricated as described in Sections 2.2.1-2.2.2; C) one section of monolith was photografted with GMA by masking the other section during exposure; D) trypsin was immobilized onto the GMA grafted monolith; E) the second section of monolith was photografted with GMA; F) Glu-C was immobilized onto the second GMA grafted monolith.

2.4 Digestion with dual enzyme reactor

Adrenocorticotropic hormone fragment 1-10 human (ACTH, 1 mg/mL in 50 mM ammonium bicarbonate, pH 7.8) digestion was conducted under constant pressure after each immobilization step described in Section 2.3.3. The digests were collected and analyzed by CE and MS.

2.5 Characterization of monolith columns

2.5.1 Scanning electron microscopy (SEM)

Samples were prepared for imaging by applying pieces of column fabricated as described in Sections 2.2.1 and 2.2.2 to sticky carbon foils on standard aluminum specimen stubs and coated with a 20 nm thick gold layer by an Edwards sputter coating unit (Crawley, West Sussex, UK). Microscopic analysis of all samples was carried out in a Hitachi S-4300 SE/N SEM (Hitachi High Technology, Pleasanton, CA, USA) operated at 5-10 kV, 100 pA probe current, and 0° tilt angle.

2.5.2 Brunauer-Emmett-Teller (BET) analysis

The poly(BAC-co-BDDA-co-AMPS) monolith was prepared in bulk using the same procedure described in Sections 2.2.1 and 2.2.2, except the polymer was prepared in a 1.5 mL UV-transparent Eppendorf tube. The polymer was then washed sequentially by ACN and methanol, dried under vacuum for 12 h. Determination of the pore size distribution profiles of the monolith was performed on a Micromeritics ASAP 2000 (Norcross, GA, USA) using nitrogen adsorption/desorption at 50 °C, and the results were calculated using the BET equation [87] (Appendix A).

2.5.3 Electrokinetic total porosity measurement

The total porosity of the monoliths was determined by the conductivity-based method proposed by Taverna *et al.* [88]. Experiments were conducted using a lab-assembled CE instrument. Electric potential was applied to the capillary by a Spellman model CZE1000R high-voltage power supply (Happauge, NY, USA). Separation voltages were controlled via a lab-written LabView 5.1 program (National Instruments, Austin, TX, USA). The mobile phase was 20 mM ammonium acetate buffer, pH 8.0. Thiourea (10 mg/mL), a neutral marker, was injected into the capillary by applying 2000 V electric voltage for 3 s. Detection was achieved with a Unicam 4225 UV detector (Mississauga, ON, Canada) that was operated at 214 nm. Data was analyzed using Igor Pro, version 3.15, from WaveMetrics (Lake Oswego, OR, USA).

2.6 Characterization of proteolytic reactors

2.6.1 Buffer preparation

All buffer solutions were filtered under vacuum through 0.45 μm nylon filters (Millipore, Billerica, MA, USA) and kept at 8 °C.

2.6.2 Quantification of immobilized proteases

The BCA reagent solution was pumped through 5 cm long, 535 μm ID monolithic columns with, and without, immobilized proteases by pressure (6.9 bar) for 1 h yielding about 600 μL. A 200 μL aliquot of the effluent was analyzed using the BCA assay according to the manufacturer's instructions.

2.6.3 Buffer pH and temperature effect

Cytochrome c (0.5 mg/mL) solutions were prepared in 50 mM ammonium bicarbonate and flushed through tryptic and Glu-C reactors under a constant pressure (6.9 bar) that produced approximately 0.4 μL/min. For the pH study (pH: 6.5 – 9.0) the digestor was held at room temperature (23 °C) but for the temperature study (23-53 °C, pH = 8.0), the reactor was immersed in a temperature controlled water bath during digestion. The digests were collected and analyzed by MALDI-MS.

2.6.4 Reactor regeneration

An inter-digestion wash for the tryptic reactor was carried out with 50 mM ammonium bicarbonate, pH 8.0 mixed with 20%, 50%, or 80% ACN at flow rate of 1 μL/min for 30 min (~60x column volumes), followed by conditioning with 50 mM ammonium bicarbonate, pH 8.0 for 10 min (~10x column volumes). The digestion performance of the trypsin reactor, using alternating cytochrome c and apo-myoglobin samples, was evaluated after each wash by continuous infusion of the sample at a flow rate of 0.5 uL/min and 22 °C. The peptides eluted from the tryptic reactor were diluted with 0.5 μL/min ACN and 0.1% formic acid through a Tee and analyzed by ESI-MS.

2.6.5 Flow rate effect

On-line cytochrome c tryptic digestions were carried out to study the effect of flow rate with the set-up shown in Figure 2-5. A Harvard Apparatus (Saint-Laurent, QC, Canada) syringe pump varied the flow rates through the digestor from 0.1-2 μL/min. After allowing the sample to pass through the digestor for 15 min, a 5 μL fixed volume of peptide solution was retained in the C18 trapping column (NanoEase™, 0.18 mm I.D. ×

23.5 mm, Waters) and eluted for ESI-MS using a 1 μL/min, 0-95% linear gradient of ACN in 0.1% formic acid over 45 min.

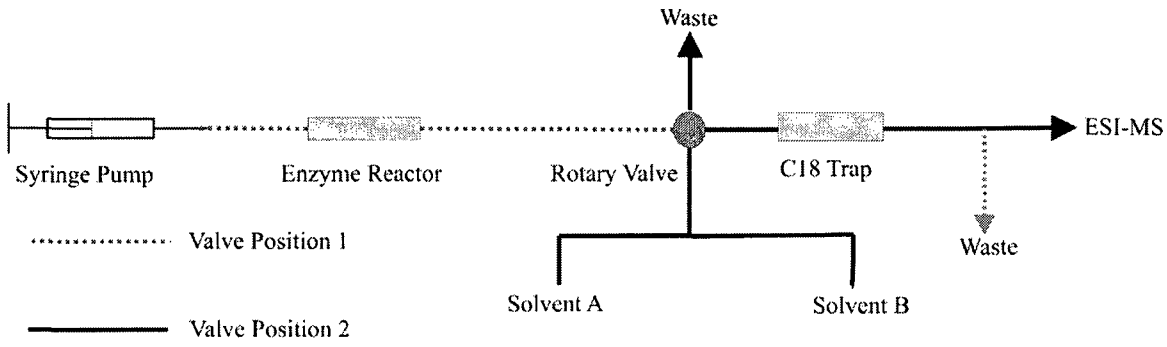

Figure 2-5: Schematic representation of the system used for on-line tryptic digestion. Solvent A was 0.1% formic acid; solvent B was 0.1% formic acid in ACN. The reactor temperature was 23 °C.

2.7 Tryptic digestion

2.7.1 In-solution tryptic digestion

Cytochrome c, apo-myoglobin, α lactalbumin and BSA (1mg/mL each) solution phase tryptic digestions (Table 1) were carried out at a protein monomer to trypsin ratio of 20:1 (w/w) at room temperature for 15 h in 50 mM ammonium bicarbonate, pH 8.0. Digestions were quenched by freezing at -80 °C. α lactalbumin and BSA were reduced with 10 μL of 100 mM dithiothreitol (DTT) and alkylated using 10 μL of 50 mM *N*-ethylmaleimide (NEM) for one hour prior to both in-solution and on-line digestions. Excess DTT and NEM were removed by centrifugal ultrafiltration (ultrafree 0.5 centrifugal filters; Millipore, Billerica, MA, USA). The protein digests were diluted 5-30-fold into 50% ACN containing 0.1% formic acid, and introduced into a Waters Micromass Q-ToF2 mass spectrometer by direct infusion.

Table 1: Properties of the four standard proteins.

Protein	Molecular Weight (Da)	pI
Cytochrome c	12,000	10.0
Apo-myoglobin	17,000	7.3
α lactalbumin	14,000	4.5
BSA	70,000	5.8

2.7.2 On-line tryptic digestion

The four proteins (Table 1) were digested by the tryptic reactor using the same experimental set-up as described in Section 2.6.5 and the results were compared to the in-solution method.

2.8 On-line protein separation and tryptic digestion

A schematic representation of combined on-line protein separation and digestion at 23 °C is shown in Figure 2-6. One half microliter of 166 μM cytochrome c and 100 μM apo-myoglobin mixture was injected into a tandem 15 cm monolithic and 10 cm digestion column (both 100 μm ID). Separation and digestion was carried out under isocratic conditions using 20% ACN in 50 mM ammonium bicarbonate, pH 8.0 at 0.5 μL/min. The peptides eluted from the tryptic reactor were diluted with 0.5 μL/min ACN and 0.1% formic acid through the Tee and analyzed by ESI-MS.

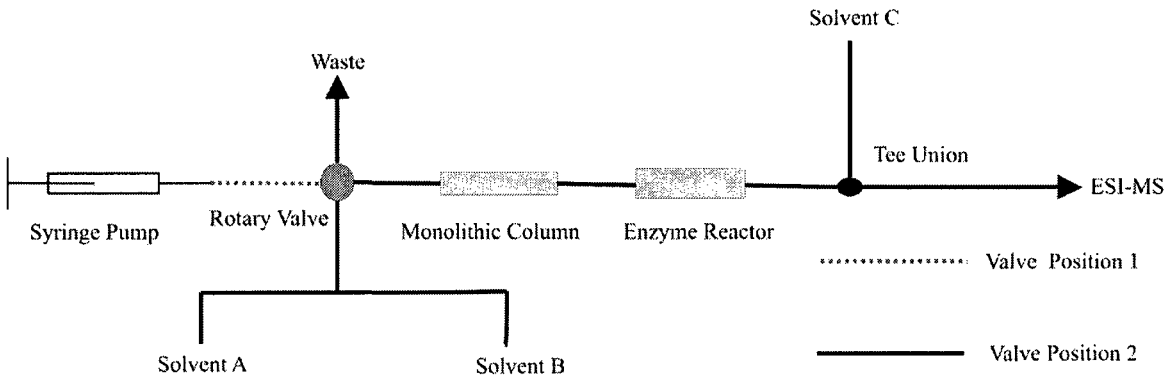

Figure 2-6: Representation of the system for on-line protein separation and digestion. Solvent A was 50 mM ammonium bicarbonate, pH 8.0; solvent B was ACN; and solvent C was 50% ACN and 0.1% formic acid. The temperature was 23 °C.

2.9 Monolith surface modification by PEG

Five monolithic reactors with varying amounts of trypsin and amino terminated PEG were fabricated as described in Section 2.3. During immobilization, 2 mg/mL mixtures of trypsin and PEG (0, 25, 50, 75, 100 wt%) were reacted with the surface.

Ten picomoles of a peptide mixture (Gly-Tyr, Val-Tyr-Val, methionine enkephalin acetate, leucine enkephalin, angiotensin II acetate) was injected into the trypsin-PEG reactors. The mobile phase was 20% ACN in 50 mM ammonium bicarbonate, pH 8.0 at 0.5 μL/min, and was mixed post-column with 0.5 μL/min ACN and 0.1% formic acid through the Tee and analyzed by ESI-MS. Cytochrome c (14 pmol) was used to study digestion efficiency of these reactors with the experimental set-up described in Section 2.6.4.

2.10 Instrumentation

2.10.1 Capillary electrophoresis analysis

Capillary electrophoresis experiments were performed using a P/ACE MDQ CE System equipped with a diode array detector (DAD) and Karat 32 software (Beckman Coulter, Fullerton, CA, USA).

2.10.2 MALDI-TOF MS analysis

Protein sequencing was performed on a MALDI-TOF mass spectrometer from Micromass (Waters Micromass) equipped with a 337 nm N_2 laser. Calibration was carried out using angiotension I (1296.5 Da), Glu-fibrino peptide (1570.6 Da), and ACTH (fragment 18 – 39, 2465.7 Da). Digested samples were desalted using C_{18} ZipTip pipette tips (Millipore, Bedford, MA, USA), and re-suspended in 1.5 μL ACN (60%) and trifluoroacetic acid (0.1%). The treated sample was then mixed with an equal volume of a solution of 50 mM α-cyano-4-hydroxy cinnamic acid in 50:50 ACN/ethanol. The room temperature dried-droplet method described by Karas [89] was used for the duplicate analysis of the samples (1 μL) deposited on a MALDI PrepTarget stainless steel plate. Data was recorded in reflectron positive ion mode.

2.10.3 ESI-Q-TOF MS analysis

ESI-MS analysis was performed on a Waters Micromass Q-ToF2 mass spectrometer equipped with a Z-spray ion source and a ternary gradient Micromass CapLC system. Mass calibration was carried out using human [Glu_1]-fibrinopeptide B, and yielded a mass accuracy of ~30 ppm in positive ion mode. The instrumental parameters are listed in the figure legends. Data analysis was performed using MassLynx

4.0 software (Waters Micromass), and peptide fingerprint searches were carried out using MASCOT (Matrix Science).

Chapter 3 Results and Discussion

3.1 Characterization of monolith columns

The morphology of monolithic stationary phases is of crucial importance when these types of stationary phase are applied to separations [90] and enzymatic digestors [80]. Bed homogeneity largely determines the separation efficiency (plate height) that can be attained for a given monolith and is one of the chief advantages of *in-situ* polymerized monoliths over similarly dimensioned packed capillary columns. The high surface area to volume ratio, and high degree of interconnected channels produced in photopolymerized monoliths provides rapid mass transfer for both large and small analyte molecules and is advantageous for both chromatographic and proteolytic digestor applications. The methacrylate-based polymer used in this thesis has demonstrated its suitability for high efficiency capillary electrochromatography (CEC) separations [85, 91] which rely on the electroosmotic flow (EOF) generated by the AMPS. Although AMPS was not directly necessary for the digestor experiments, it was maintained in the polymer recipe so that the morphology of the base polymer would not be altered compared to previous reports [85, 91] and would be available to provide EOF in electro-driven applications, even after photografting [92]. In order to evaluate physical and chemical properties of the monolithic stationary phases, SEM, BET nitrogen adsorption-desorption isotherms, and total porosity measurements were carried out.

3.1.1 Scanning electron microscopy analysis

Several techniques, such as SEM, mercury intrusion porosimetry (MIP), Brunauer-Emmet-Teller (BET), Barrett-Joyner-Halenda (BJH) gas adsorption-desorption isotherms, and atomic force microscopy (AFM), are commonly used to investigate the

morphology of monoliths. Among them, SEM is the most widely applied imaging method in which a focused electron beam scans the surface resulting in the emission of secondary-electrons that are collected by electro-optical lenses. Detailed structures that are smaller than 50 nm cannot be resolved by SEM [93]. Validation of the morphology, by SEM imaging, is critical since slight variations in experimental factors such as irradiation source, light intensity and capillary temperature can dramatically affect the size of the microglobules and the pore size distribution [94].

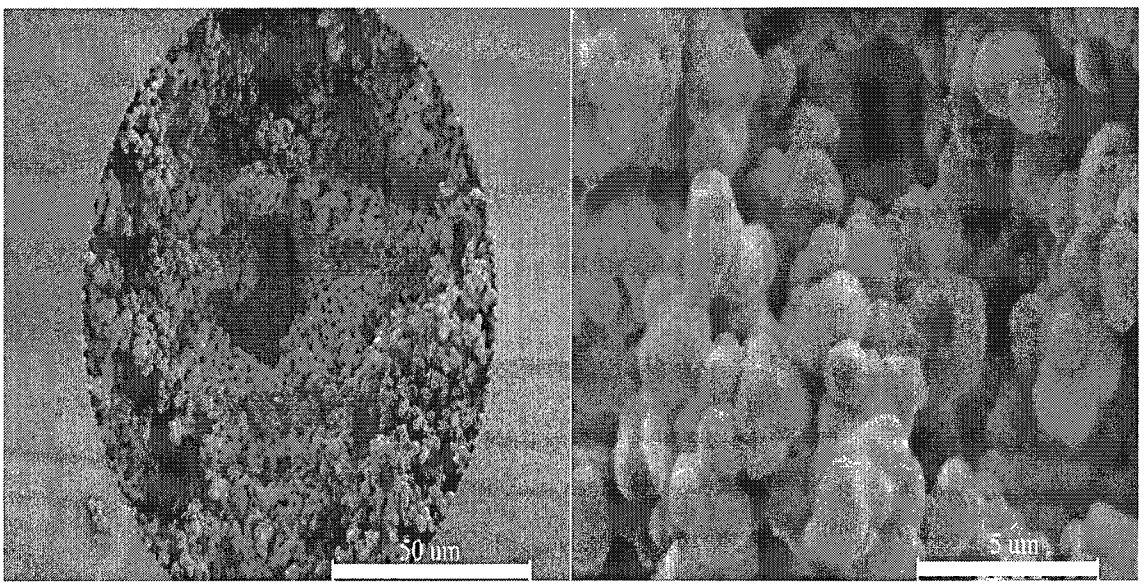

Figure 3-1: Electron micrographs of the cross-section of a monolith in a 100 μm ID capillary. Magnification: 900 x (left) and 3000 x (right).

The key aspects to producing a successfully modified monolith are the ability to incorporate the desired functional groups onto the surface without altering the basic morphology of the monolith. Figure 3-1 shows that the cross-section of the photopolymerized monolith fabricated is homogeneous across the capillary and that the silanization step anchored the monolith to the capillary wall. Silanization of capillary wall is critical since it attaches the monolith in the capillary providing good mechanical

strength even when subjected to high pressure. Failure in silanization (Figure 3-2) not only results in the detachment of the monolith from the capillary wall, and ultimately its extrusion, but also results in poor, or even no analyte interaction with the stationary phase. As can be seen from the SEM image, the majority of the analytes, in this case, would just simply bypass the stationary phase through the huge gap between the monolith and the capillary wall.

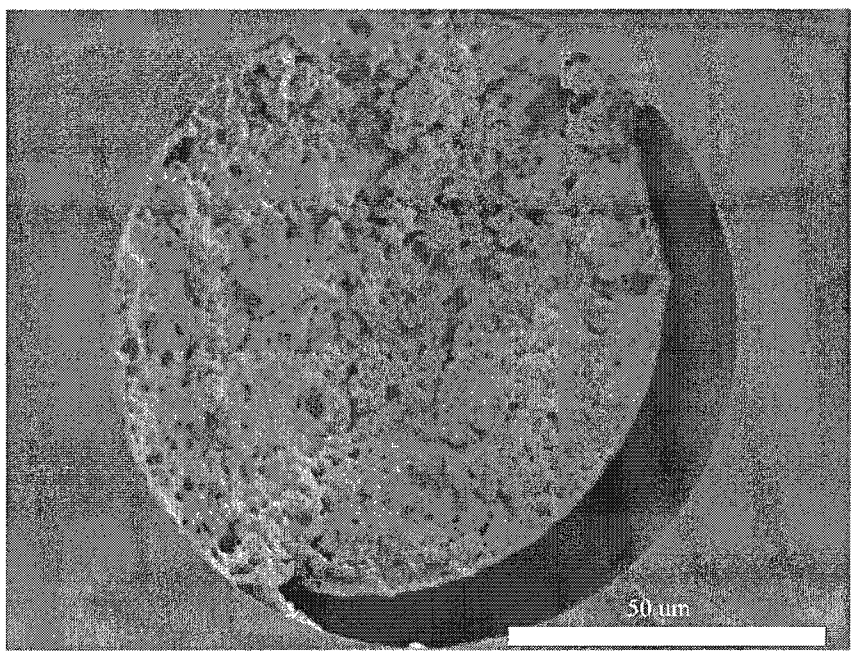

Figure 3-2: Electron micrograph of the cross-section of a monolith from a failed silanization. Magnification: 900 x.

Although it is not easily visible at the 900X magnification in Figure 3-1, the wall is covered in a skin of polymer and the majority of the wall surface is populated with polymer nodules/agglomerated microglobules. This complete coating and roughness should reduce wall-bed bandbroadening and silica-analyte interactions.

The average microglobule size determined from the SEM images was approximately 1 µm and is similar to those prepared by Ngola with the same type of

monolith [85]. Images obtained from the GMA photografted polymer (not shown) show no visible changes in morphology compared to the base monolith.

3.1.2 BET nitrogen adsorption-desorption isotherms

The pores in a porous material are classified into four classes depending on their size: ultramicropores (pore < 0.7 nm), micropores (0.7 nm < pore < 2 nm), mesopores (2 nm < pore < 50 nm), and macropores (pore > 50 nm) [95]. Macropores enable liquid to flow through the porous material at reasonable pressures, but contribute very little to the surface area that analytes can interact with. Micropores and mesopores provide the majority of the active surface area, but micropores are not accessible to large biomolecules, such as proteins, due to the size hindrance effect. Therefore, an ideal monolith should contain both large pores for convective flow and an inter-connected network of smaller pores for interaction between functional groups on the stationary phase and analytes. SEM can show the overall morphology and macropore structures of monoliths, but it cannot resolve the pores smaller than 50 nm. Hence, it is unsuitable for characterization of mesopores. Nitrogen adsorption-desorption isotherms is one of most widely used techniques based on the model developed by Brunauer, Emmet, and Teller for the physical characterization of solid substrates. This technique relies on probe gas molecules, nitrogen in this case, to adsorb to and desorb from the surface of a porous material. The adsorbed volume of the nitrogen which is assumed to be equal to that of the pores, is calculated using the BET equation [95]. When it is applied to porous materials, BET analysis can provide information on the surface area, the total pore volume, and the pore size distribution.

Our former group member, Jean-Louis Cabral performed the BET measurements on the poly(BAC-co-BDDA-co-AMPS) monolith, but unfortunately only erratic data were obtained [92]. He speculated that the conditioning temperature used to clean the sample prior to BET analysis was too high, resulting in irreversible modification of the polymer. In the present experiments, heat was not applied in the sample preparation step; instead, the sample was placed *in vacu* for 12 hours before the analysis in order to remove any adsorbed liquid and air trapped within the solid porous network.

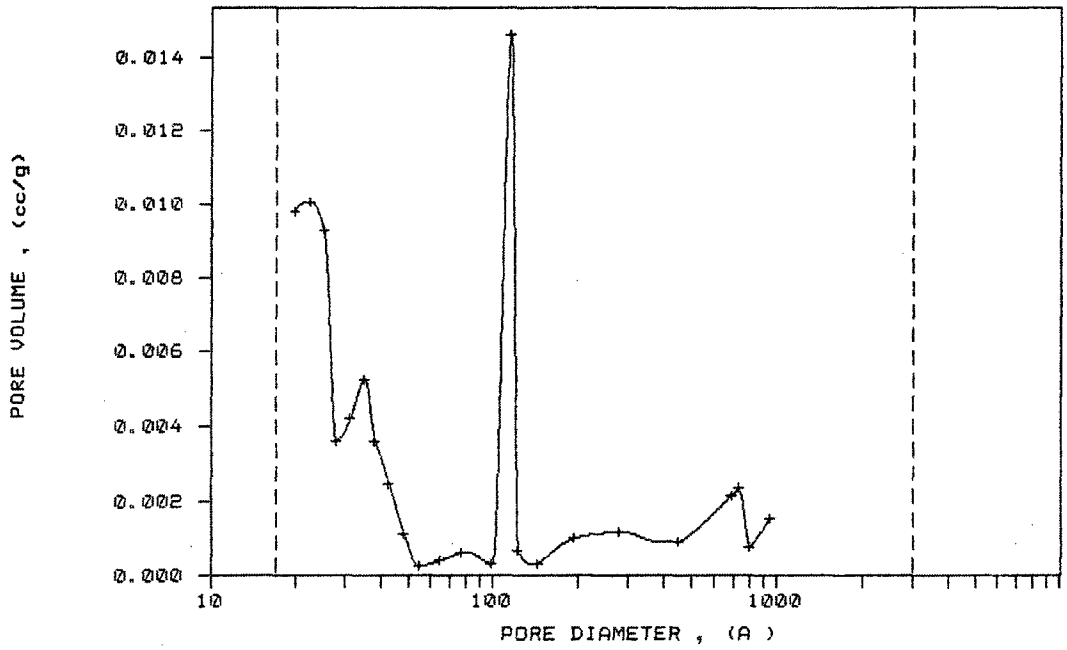

Figure 3-3: Pore size distribution of the poly(BAC-co-BDDA-co-AMPS) monolith by BET.

In Figure 3-3, a bimodal pore size distribution in the range of 1 to 100 nm was observed. The first set of pores with pore diameters smaller than 50 Å provided the majority of surface area. These small pores and the corresponding large surface area are essential for small molecule chromatography as they allow the small molecules to diffuse into the pores and to interact with the functional groups on the surface area of the

stationary phase. The mesopores with pore diameters from 100 to 800 Å are the primary sites in which large molecules, such as proteins, can interact with the stationary phase. It is acknowledged that effective stationary phases should possess a pore size diameter at least 10 times the protein hydrodynamic radius in chromatography [96].

It is worth noting that the BET experiment was conducted using dry monolith samples, so the data obtained may not represent the exact physical state of the monoliths in working conditions (wetted). However, the "dry" values are still informative, and can be used to tailor column performance, since a strong correlation exists between the "dry" porous properties of the monoliths and their chromatographic performance [97].

3.1.3 Electrokinetic total porosity measurement

While SEM and BET evaluate the overall morphology and pore size distribution of the monoliths in the dry state, the total porosity of the monoliths can be assessed in the wetted working state. Total porosity is the ratio of the volume of the pores within the monolith to the volume of the monolith. The porosity is useful because it provides information on the effective portion of the stationary phase that participates in the interaction with the analytes. Low porosity values are also indicative that high backpressures can be expected with hydrodynamic flow.

In this work, the total porosity of the monoliths was determined by the conductivity-based method proposed by Taverna *et al.*[88] (Appendix B). This method relates total porosity (ε_T) to the conductivity ratio between a monolithic capillary column and an open capillary corrected for length and the data is shown in Table 2.

Table 2: Porosity parameter calculated based on Taverna's method.

Method	Equation	Porosity (dimensionless)
Taverna	$\varepsilon_T = \frac{L_e \emptyset}{L_{pack}}$	0.62 ± 0.08

L_{pack} and L_e are, respectively, the packed length of the capillary column and the effective flow path length. ϕ represents the conductivity ratio of the packed segment and of the open capillary.

The porosity value is comparable to those generally reported for HPLC columns and acrylate-based monolithic columns (0.5 – 0.8) [98]. Unlike other conductivity-based methods for porosity, Taverna's method takes into account the tortuosity by introducing the effective flow path length (L_e). L_e is the actual length that the flow travels in the column. The value of L_e is higher than that of column length, which is related to the fact that any given element of mobile phase must travel a tortuous path through the stationary phase. This method appears to provide the best fit of the experimental data when dealing with columns with small d_{pore}, like acrylate-based monoliths [88].

3.1.4 Separation of standard peptides

High efficiency separations of model proteins and small hydrophobic molecules have been demonstrated using the poly(BAC-co-BDDA-co-AMPS) monolithic columns in CEC with UV detection [85, 91, 92]. In order to show the versatility of this monolithic stationary phase, separations of model peptides (Table 3) in the pressure-driven gradient mode were conducted. Moreover, separations of large biomolecules (proteins) were also performed and are demonstrated in Section 66

Table 3: Properties of the five standard peptides.

Peptide	Sequence	Molecular Weight (Da)
Gly-Tyr	GY	238.2
Val-Tyr-Val	VYV	379.5
Methionine Enkephalin	YGGFM	573.7
Leucine Enkephalin	YGGFL	555.6
Angiotensin II	DRVYIHPF	1046.2

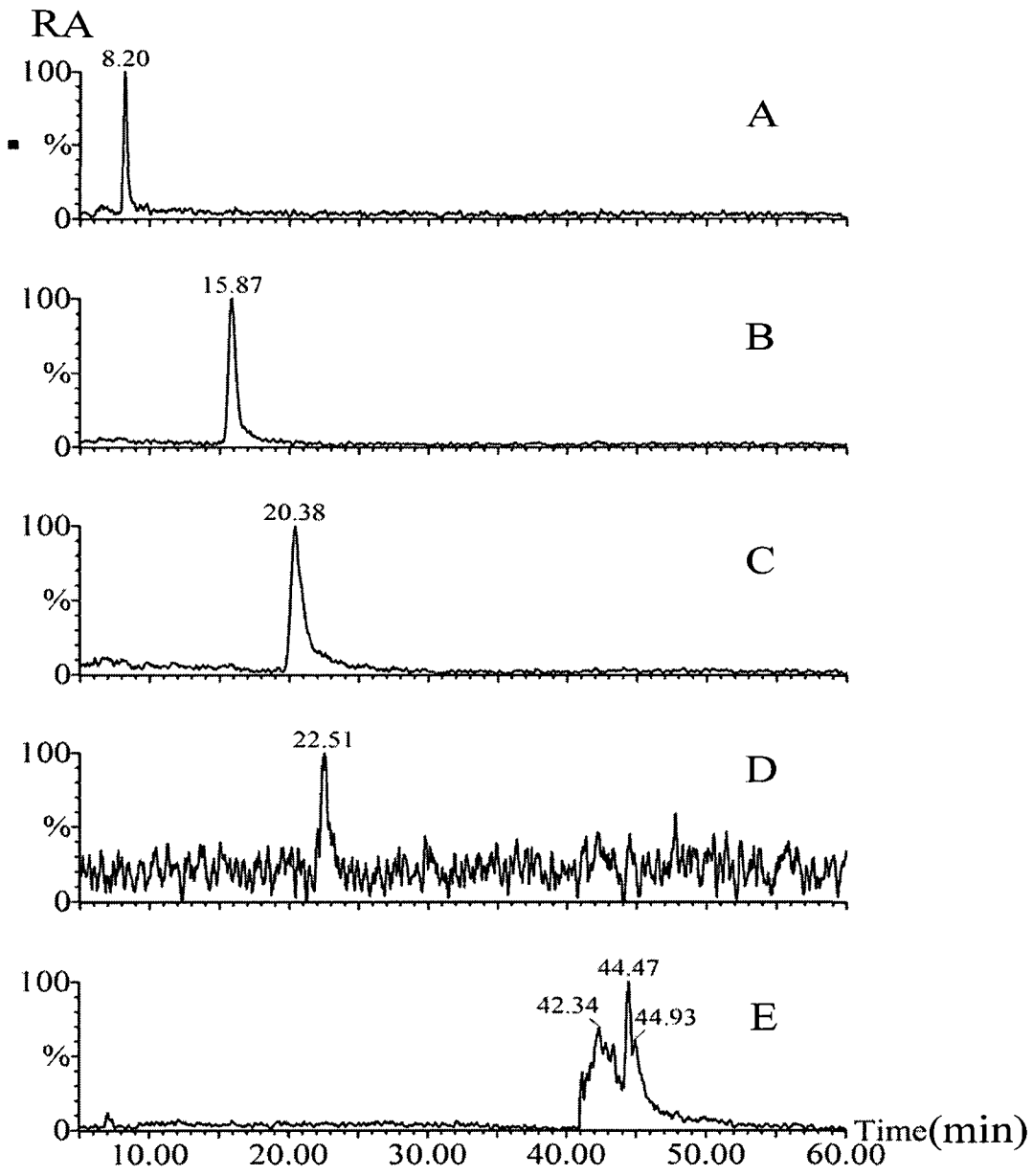

Figure 3-4: Total ion current chromatograms of separation of a standard peptide mixture using a poly(BAC-co-BDDA-co-AMPS) monolithic column. The peptide mixture (total 1 pmol) was injected into the monolithic column (15 cm, 100 μm ID), and eluted using a 1 μL/min, 0-90% linear gradient of ACN in 0.1% formic acid over 60 minutes at 22 °C and detected by ESI-MS. The peaks were identified: A) Val-Tyr-Val; B) Methionine enkephalin; C) Leucine enkephalin; D) Angiotensin II; and E) Gly-Tyr. RA is the relative abundance of the ions.

Without tuning the separation conditions, *e.g.* mobile phase composition, pH, temperature, these five peptides were baseline separated. However, peak tailing and distortion were observed, indicating that the solvent (HPLC water) for the sample may not be ideal, and a buffer solvent, such as ammonium acetate, should be used to improve the peak symmetry. The five peptides are different in their hydrophobicity and size. Methionine enkephalin and leucine enkephalin (peaks B and C) have very similar sequences, with the only difference being from the non-polar lateral chains in the last amino acid. However, even with such a subtle difference, the separation efficiency was high enough to differentiate these and all of the peptides. Interestingly, the order of elution of these peptides was not as predicted from their hydrophobicity. Val-Tyr-Val (peak A), the most hydrophobic peptide, eluted first while angiotensin II (peak D), the least hydrophobic peptide, eluted second to last. This suggests that the separation mechanism from the poly(BAC-co-BDDA-co-AMPS) monolith was not exclusively reversed-phase. The possible explanation is a combined reversed-phase chromatography and ion-exchange mode contribution from the AMPS functional groups on the surface. Further systematic studies are required to ascertain the precise retention mechanisms. Due to the limited time of this project, investigation of the retention mechanisms is not included in this thesis.

3.1.5 Summary of monolith characterization

SEM showed excellent bed homogeneity of the poly(BAC-co-BDDA-co-AMPS) monolithic stationary phase prepared in capillary columns. The data obtained from both BET and electrokinetic total porosity measurement suggested that the monolith is a highly porous material containing a large amount of micropores as well as mesopores.

As the results indicate, the high degree of interconnected channels in this photopolymerized monolith provides rapid mass transfer for analyte molecules and is advantageous for both chromatographic and proteolytic digestor applications.

3.2 Characterization of proteolytic reactors

There are several routes to preparing monolith-based enzymatic reactors but photografting has demonstrated its capacity to produce well-defined monoliths with a wide variety of surface chemistries [71]. This technique permits controlled introduction of specific surface functionalities onto the monolith that may be difficult to achieve when these same functionalities are incorporated into the pre-polymerization monomer mixture. By taking advantage of this unique feature of photografting, both trypsin and Glu-C have been immobilized onto the monolith, but any number of other molecules could also have been immobilized (*e.g.* antibodies, aptamers, chiral selection moieties *etc.*). Since the immobilization process may affect the overall protease activity and specificity, characterization of the proteolytic reactors was conducted.

3.2.1 Quantification of immobilized proteases

In this work, quantification of the immobilized protease, using the bicinchoninic acid (BCA)-containing protein assay, was made on larger 535 μm ID reactors because the smaller 100 μm ID reactors did not produce sufficient product (Cu^{+}) for quantification. The BCA assay consists of reduction of Cu^{2+} to Cu^{+} by protein in an alkaline medium in the first step and colorimetric detection of the cuprous cation by bicinchoninic acid in the second step (Figure 3-5). The first step is also known as the Biuret reaction in which peptides containing three or more amino acids form a chelate complex with Cu^{2+} in alkaline condition, producing Cu^{+}. In the second step, the intensity of the color produced by the bicinchoninic acid and Cu^{+} complex is proportional to the number of peptide bonds participating in the reaction. The theoretical detection limit of this assay is about

5 μg/mL, and the linear working range using BSA as a substrate is from 20 – 2000 μg/mL, according to the manufacturer.

STEP 1. (Biuret Reaction)

$$\text{Protein} + Cu^{2+} \xrightarrow{OH^-} Cu^{1+}$$

STEP 2.

Cu^{1+} + 2 Bincinchoninic acid (BCA) ⟶

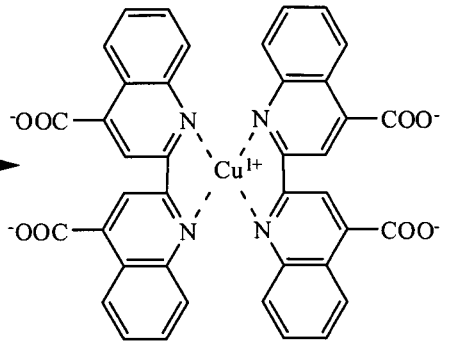

Figure 3-5: Reaction schematic for the BCA protein assay.

The BCA assay showed that 340 ± 140 μg of trypsin were immobilized per 1 g of support while 320 ± 140 μg/g support was immobilized on the Glu-C column (Table 4). This is in sharp contrast to preliminary results where 5.8 mg trypsin /g of monolith were obtained using the absorbance based method in which the difference between initial amount of protease in the reaction medium and any protease recovered after the immobilization reaction was measured. The three reports in the literature that used the absorbance based method found 7.75 mg trypsin /ml polymer [76], 2.9 – 7.1 mg papain /g support [24], and 4.9 mg trypsin /g controlled pore glass [99]. The disparity between the absorbance and BCA results cannot be reconciled, but the BCA assay directly probes the protein immobilized on the monolith whereas the absorbance based assay measures the difference in the immobilization protein concentration and assumes that all of that protein is immobilized, a potentially tenuous assumption.

Table 4: Quantification of enzyme immobilized on 535 μm ID columns and normalized to a 100 μm ID column.

	Trypsin	Glu-C
Enzyme Mass (μg/535 μm ID column)	10.2 ± 4.2	9.45 ± 4.2
Enzyme Mass (μg/g polymer) (on 535 μm ID column)	339 ± 140	315 ± 140
Expected Enzyme Mass (μg/100 μm ID column)	1.02 ± 0.43	0.950 ± 0.43
Enzyme: Protein (g/g) (at 0.5 mg/mL protein)	3 : 1	3 : 1

One of the most important parameters that affects proteolytic digestion speed and efficiency is the enzyme to substrate ratio. With in-solution digestion this ratio is trivial to control and is fixed at the frequently used value of 1:20. Assuming that the results from the BCA measurements are correct the protease to protein ratio was 3:1 for the reactors. This relatively high local concentration of the protease ensured that the reactor enzymatic digestions were faster than the in-solution digestion while producing comparable sequence coverages.

3.2.2 Immobilized protease activity

The methods to measure the activity assay of free, or immobilized, proteases are well documented in the literature [20, 24, 100, 101]. The protease activity assay is carried out by mixing the increasing concentrations of substrate with fixed amounts of enzyme. The reaction rate is elucidated by monitoring the amount of product released and measuring at a specific wavelength spectrophotometrically. For the trypsin activity assay, substrates of low molecular weight containing an arginine cleavage site, such as N-α-benzoyl-L-arginine ethyl ester (BAEE) and N-α-benzoyl-DL-arginine p-nitroanilide (BAPNA), are commonly utilized. This assay for free trypsin is simple to perform and has become a routine experiment in research labs. A more sophisticated method, used to

assay immobilized trypsin, employs a chromatographic system consisting of an injector, a pump, a trypsin reactor, and a UV detector. In this assay, substrate solutions at increasing concentration are injected into the system at a fixed flow rate and peaks of the proteolytic product are monitored at a specific wavelength. The kinetic parameters, V_{max} and K_m, are calculated from the Michaelis-Menten and Lineweaver-Burk plots based on the rate of enzymatic reaction (expressed as Δarea product/min) and the substrate concentration [100]. The activity of both free and immobilized Glu-C can also be assessed using the same methods just with different substrates.

Two different substrates were tested to evaluate the proteolytic activity of immobilized trypsin. The first one was BAPNA, but no product was detected. The lack of elution was thought to be due to strong interaction between the products with the monolith. This result was also reported by Jean-Louis Cabral in his thesis [92]. The second substrate was green fluorescent protein (GFP) which is a 29 kDa monomer with Ex/Em = 488/507 nm [102]. GFP has a unique structure, similar to a soda can covered by a beta-barrel with the chromophore located in the middle of the beta-barrel. The fluorescence intensity decreases as the barrel is destroyed, by *e.g.* proteolytic digestions. In the experiment, however, the fluorescent intensity of GFP incubated with various amounts of free trypsin (from 1:10 to 1:1) stayed constant during the course of each 5 minute digestions. The fact that GFP is very resistant to proteolytic digestions implies that extended incubation times would be required to measure immobilized enzyme activity.

Since no suitable substrate has been found, the activity assay of immobilized proteases was not included in this thesis. However, this experiment still remains of interest to our lab, and will be performed as soon as a viable substrate is determined.

3.2.3 Buffer pH and temperature effect

It is well known that enzyme activity in solution is largely influenced by several key parameters, such as buffer composition, pH, digestion time, and digestion temperature. It has been reported that the optimal buffer pH and digestion temperature for trypsin are pH 8.0 and 37 °C [103] while for Glu-C a pH 7.8 and 37 °C [84] are optimal. Compared to their counterparts in solution, immobilized enzymes might have different values for those parameters due to the influence of the immobilization process (restraint on conformational change and rotation of enzymes, steric hindrance of active sites, *etc.*) and the unique properties of stationary support such as the electrical double layer established by the AMPS. Thus, the digestion performance of both immobilized trypsin and Glu-C reactors in 50 mM ammonium bicarbonate, pH 6.5 – 9.0, at 23 °C and 23 – 53 °C but at a fixed buffer pH of 8.0 was investigated. Both experiments were performed with a constant flow rate of 0.5 μL/min using cytochrome c as a test substrate, and digests were collected and analyzed by MALDI-MS.

Table 5: Sequence coverage (percent) of cytochrome c as a function of pH and temperature.

Buffer pH			Temperature		
pH	Trypsin	Glu-C	Temperature (°C)	Trypsin	Glu-C
6.5	N/A	8	23	60	17
7.0	68	26	33	60	26
7.5	69	28	37	76	26
8.0	81	28	43	77	28
8.5	82	20	50	69	28
9.0	67	N/A			

Table 5 shows that the optimal pH for immobilized trypsin was from 8.0 – 8.5, which agrees with that reported for in solution digestion and with those observed from trypsin immobilized on porous monoliths [67, 82] and on porous glass [99]. The Glu-C reactor showed a wider optimal pH range than trypsin with relatively good digestion efficiency between pH 7.0 and 8.0 that compares well with the reported in-solution efficiency at pH 7.8. A relatively flat temperature profile for both immobilized trypsin and Glu-C was observed with uniform sequence coverages obtained between 33 and 43 °C for trypsin and 37 to 50 °C for Glu-C. The lower than expected sequence coverage of the Glu-C digestor (<30%) was surprising but can be explained by the realization that the digestor's selective cleavage at glutamic acid should produce a 4470 Da peptide that represents 40% of the cytochrome c sequence (see the expected peptides in Appendix D), but the MS scan parameters only allowed peptides up to 3000 m/z to be detected and apparently prevented detection of this particular peptide. These two studies suggested that the basic properties of these two proteases were not altered by the immobilization process and are in agreement with trypsin immobilized on other supports using different chemistries [101, 104, 105].

3.2.4 Flow rate effect

Successful, continuous on-line protein digestion using proteolytic reactors is largely dependent on flow rate, since it determines the contact time between the substrate and the protease within the reactor. Therefore, an investigation of the effect of flow rate on protein digestion in tryptic reactors using cytochrome c as a model protein was carried out (Figure 3-6) with the experimental set-up shown in Figure 2-5.

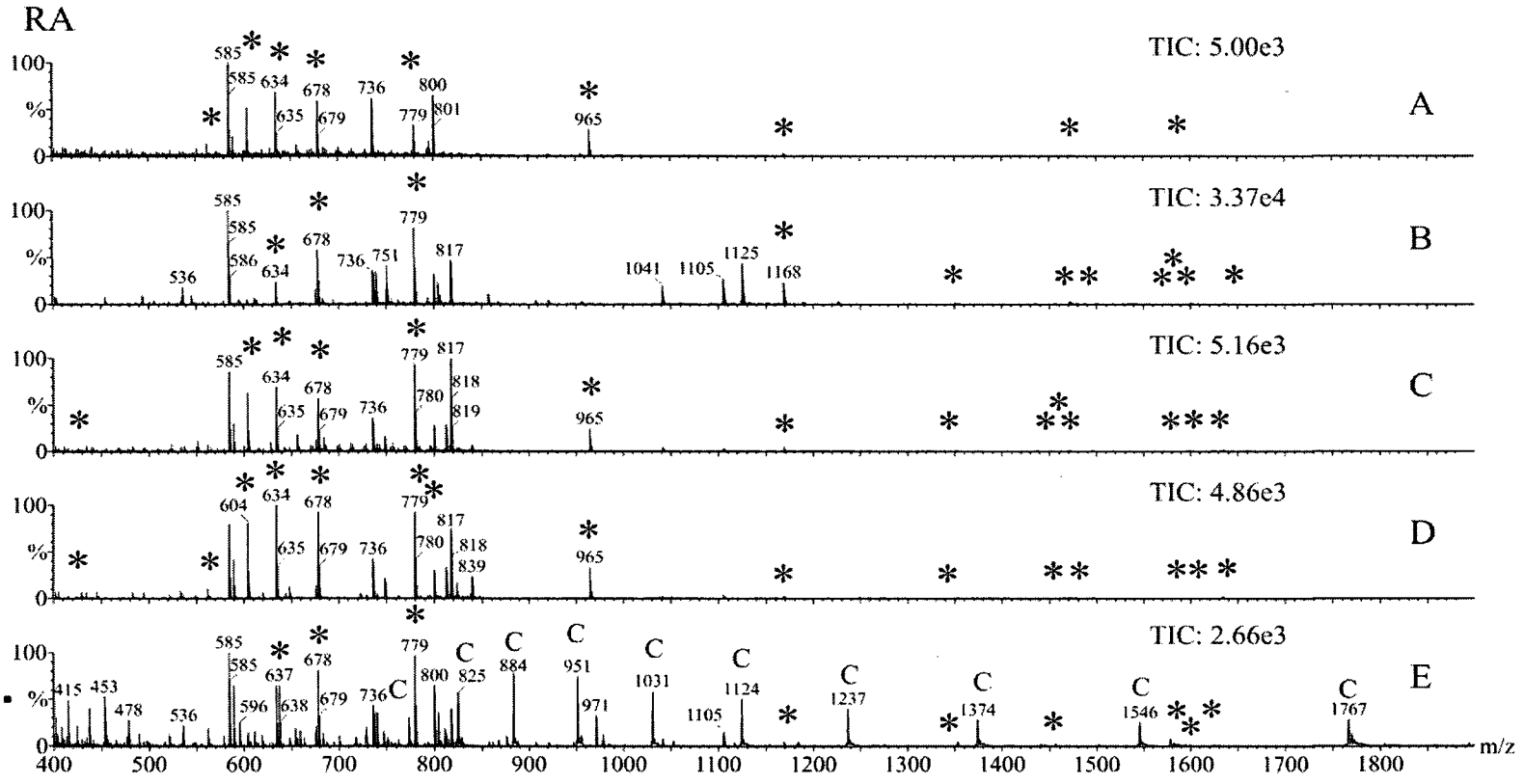

Figure 3-6: On-line tryptic digestion of 0.5 μg/μL cytochrome c in 50 mM ammonium bicarbonate, pH 8.0, at various flow rates. A) 0.1 μL/min, B) 0.3 μL/min, C) 0.5 μL/min, D) 1.0 μL/min, and E) 2.0 μL/min. For MS analysis, the instrumental parameters were as follows: source block temperature, 80 °C; capillary voltage, 3.5 kV; cone voltage, 35 V; collision voltage, 10 V (no collision gas); TOF, -9.1 kV; MCP, 1.8 kV. RA is the relative abundance of the ions, and TIC is total ion count. Identified peptides are labelled with *, and the intact protein envelope is labelled with C.

The calculated contact time at each flow rate, listed in Table 6, is based on a monolith total porosity of 0.6 determined from conductivity measurements described in Section 3.1.3. At the lowest flow rate measured, 0.1 μL/min (Figure 3-6A), all the peptide ions identified were free of missed cleavages except for ions at *m/z* 562 and 1598. The low flow rate allowed the longest contact time, therefore, resulting in a more complete digestion, but at this flow rate, peptides with significant retention were not successfully eluted. As the flow rate was increased (0.3-1 μL/min), more peptide ions were observed, and consequently sequence coverage increased from 60% up to 87%. However, the number of peptides with missed cleavages also increased from 2 to 7 suggesting that there was insufficient contact time to allow complete digestion. For the digestion at the highest flow rate (2 μL/min, Figure 3-6E), intact protein ions and large peptide ions with missed cleavages were dominant in the spectrum. At these high flow rates, the inefficiency of diffusive mass transport of the substrate to the enzyme significantly limited the enzymatic reaction. Incomplete digestion is undesirable since the presence of the intact protein ions not only competed with peptide ions for ionization, but also complicated analysis of the MS spectrum. As a result, both the peptide signal intensity and the signal to noise ratio decreased resulting in a modest sequence coverage of 62%. No MS/MS sequencing was required for the positive identification of the peptides since the mass error was around 30 ppm. The optimal flow rate for cytochrome c digestion was 0.5-1 μL/min. but the optimal flow rate for digestion of other proteins may be different. The flow rate for on-line protein digestion using proteolytic reactors should be tuned prior to the analysis based on the substrate's size and structure. In

general, digestion of substrates with high molecular masses or those that are resistant-to-digestion require lower flow rates.

Table 6: Overview of on-line cytochrome c digestion with immobilized trypsin at different flow rates.

Flow Rate (µL/min)	0.1	0.3	0.5	1	2
Contact time (s)	282	94.2	56.4	28.2	14.4
Peptide *m/z*	MC*	MC*	MC*	MC*	MC*
261	0		0	0	
332			1	1	
405				0	
434			0		
562	1			1	
604	0		0	0	
634	0	0	0	0	0
678	0	0	0	0	0
779	0	0	0	0	0
806		1		1	
964	0		0	0	
1168	0	0	0	0	0
1350		1	1	1	1
1470	0	0	0	0	
1478		2	2		2
1495			0	0	
1598	1	1	1	1	1
1606		3			3
1623			1	1	
1633		1	1	1	1
1712		1			
Sequence Coverage	60%	73%	87%	82%	62%

*MC is the number of missed cleavages in the detected peptide. An empty cell means that the peptide was not detected at that flow rate. Note, not all of the expected tryptic peptides are listed.

3.2.5 Reactor regeneration

One of the advantages that proteolytic reactors possess is that they can be reused for a number of times and the digestion efficiency of these reactors can be maintained for a long period of storage time. It was observed that both trypsin and Glu-C reactors after two months of storage at 8 °C yielded similar digestion performance as newly synthesized microreactors. One of the factors that lengthens the reactors' life cycle is using an effective washing method to elute the built-up peptide fragments and undigested proteins from the previous digestion cycle, providing a "clean" reactor without any carry-over for the next cycle. An appropriate inter-digestion wash for the hydrophobic monolith was sought by using ammonium bicarbonate buffer solutions mixed with increasing amounts of ACN. The digestion performance of the trypsin reactor, using alternating cytochrome c and apo-myoglobin, was evaluated after each wash. The results are presented in Figure 3-7.

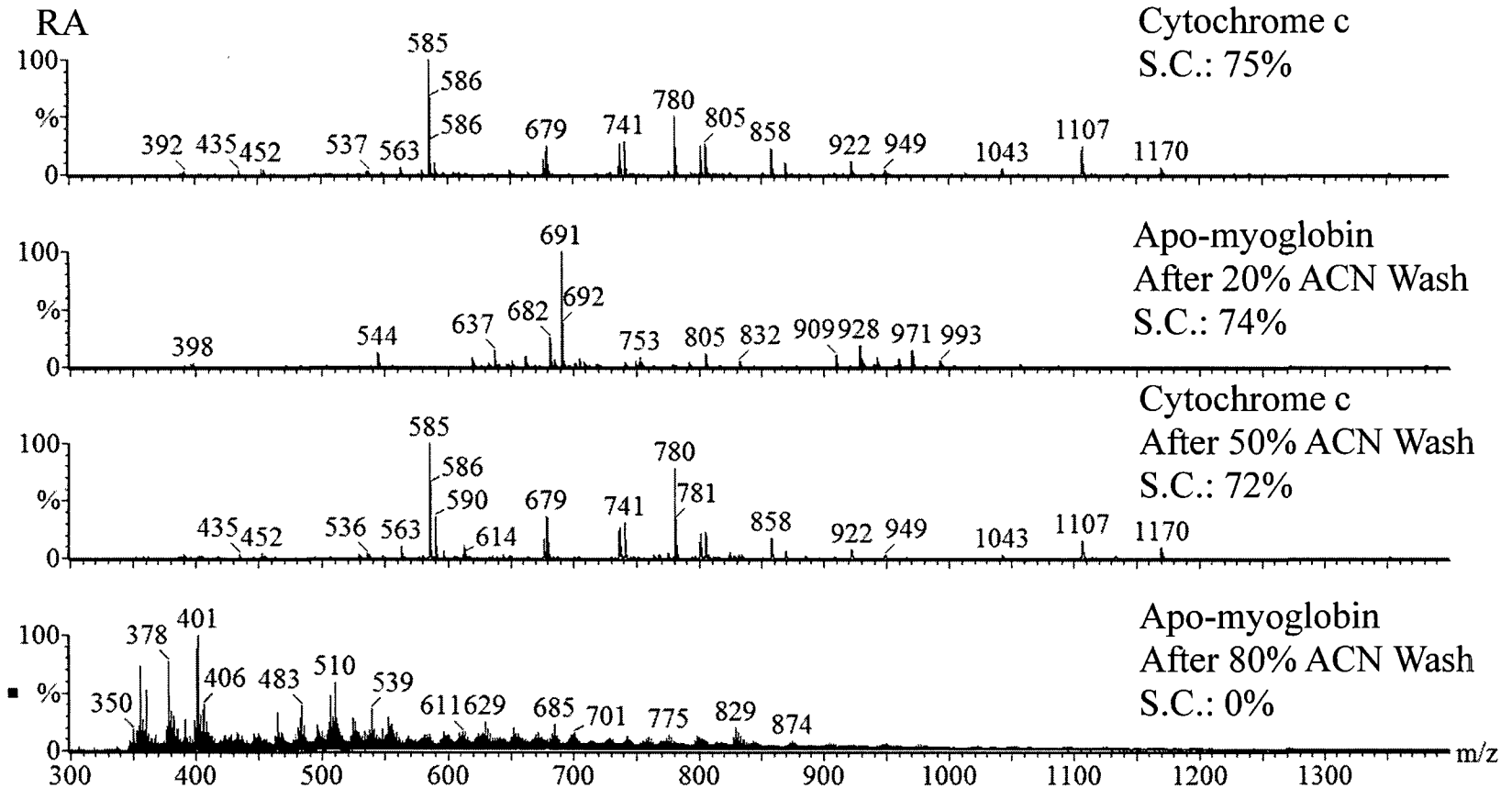

Figure 3-7: On-line tryptic cytochrome c and apo-myoglobin digestions after washing. From top to bottom, A) cytochrome c digestion; B) apo-myoglobin digestion after 20% ACN wash; C) cytochrome c digestion after 50% ACN wash; and D) apo-myoglobin digestion after 80% ACN wash. Mass spectra are from an accumulation of 60 seconds of data. RA is the relative abundance of the ions.

By using a long wash and alternating the protein digested, it was possible to demonstrate that no new peptides (not observed in the digest) were detected in the wash, and that no peptides were carried-over, from the previous digestion. Later in the thesis, it will be shown that, in general, all of the peptides are coeluted from the column independent of hydrophobic characteristics. The trypsin reactor was irreversibly and completely deactivated after exposure to wash solutions with more than 50% ACN. The literature suggests that the immobilized trypsin is denatured by high organic fractions, leading to the loss of its activity [106]. Trypsin, a 24 kDa protein, is incapable of successful spontaneous refolding [107] and refolding may have been further hampered by proximity to the hydrophobic supporting monolith.

Based on the data from this experiment and from 3.3.1, washing after each digestion was carried out using 50 mM ammonium bicarbonate, pH 8.0 with 20% ACN for 15 minutes throughout this thesis work, but much shorter washing times may be possible and deserves further investigation.

3.2.6 Standard protein digestion by in-solution and on-line tryptic digestion

Four proteins, with molecular masses from 12 to 70 kDa and pI's from 4.5 to 10.0, were digested by the tryptic reactor and compared to the in-solution method to demonstrate that the reactors were capable of digesting a wide variety of proteins. The experimental set-up for on-line digestion is shown in Figure 2-5 with the digestion results presented in Figure 3-8 to Figure 3-11.

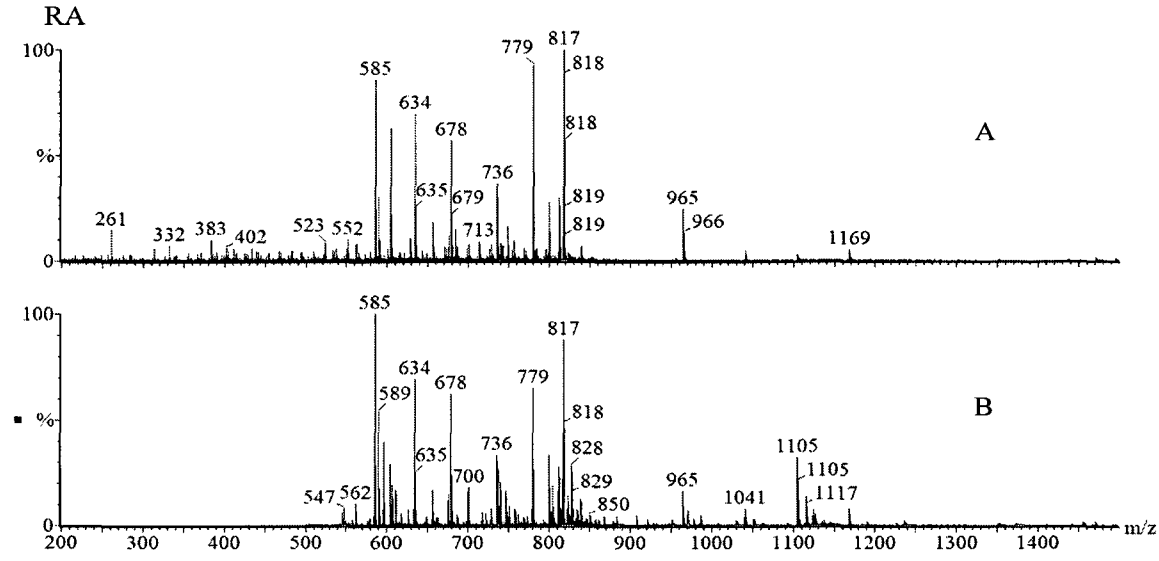

Figure 3-8: MS spectra of tryptic digestion of cytochrome c. A) On-line digestion; B) In-solution digestion. For MS analysis, the instrumental parameters were as follows: source block temperature, 80 C; capillary voltage, 3.2 kV; cone voltage, 30 V; collision voltage, 5 V (no collision gas); TOF, -9.1 kV; MCP, 1.8 kV. RA is the relative abundance of the ions.

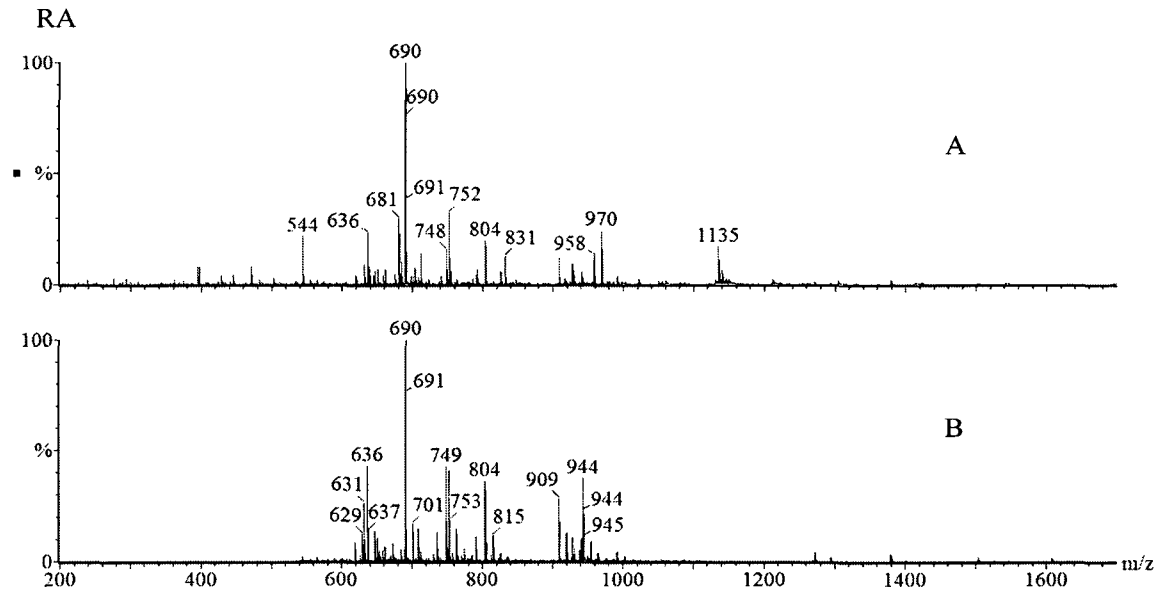

Figure 3-9: MS spectra of tryptic digestion of apo-myoglobin. A) On-line digestion; B) In-solution digestion. The MS experimental conditions are given in the caption of Figure 3-8.

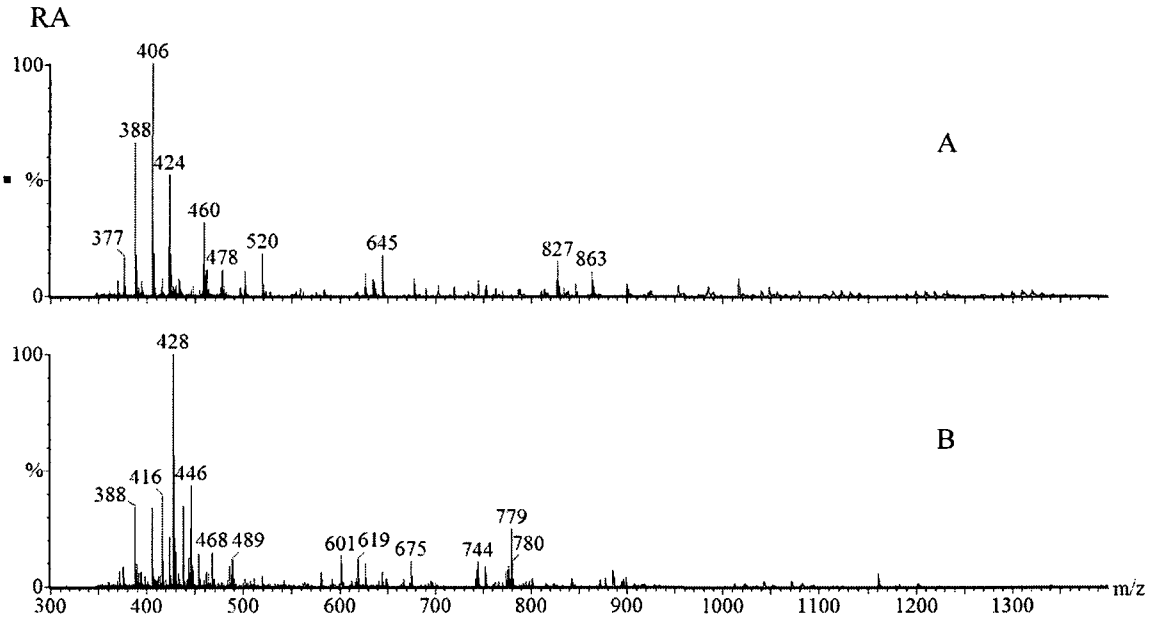

Figure 3-10: MS spectra of tryptic digestion of α lactalbumin. A) On-line digestion; B) In-solution digestion. The MS experimental conditions are given in the caption of Figure 3-8.

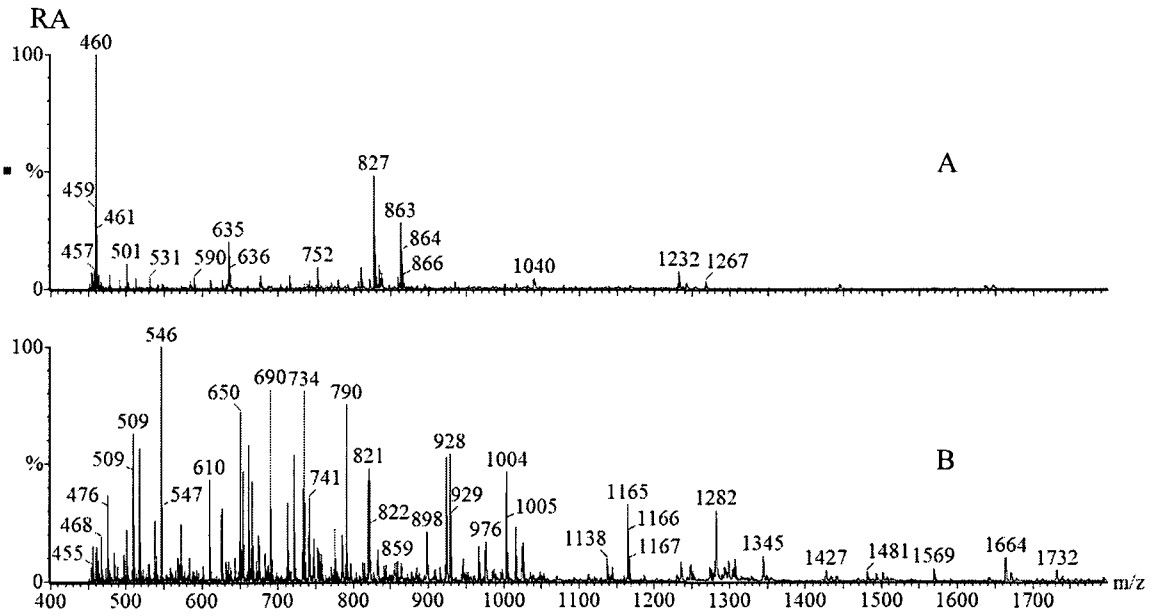

Figure 3-11: MS spectra of tryptic digestion of BSA. A) On-line digestion; B) In-solution digestion. The MS experimental conditions are given in the caption of Figure 3-8.

The salient points from these experiments are that the digestor produces sequence coverages from 43-85% with less than two and a half minutes of contact and can produce

peptides not observed with in-solution digestion (Figure 3-12). The larger proteins did not produce as large sequence coverages as the smaller proteins. Higher BSA sequence coverage using immobilized trypsin and a 4-8 min digestion time, has been reported in the literature [108, 109], but in our experiment, the digestion time was 1.4 min. It suggests that in general large and/or resistant-to-digestion substrates require longer contact times and that a compromise flow rate would have to be found in the case where multiple proteins were to be digested. In all cases, protease autolysis products were absent in the digestates. This compares very favourably with the in-solution digestion which required approximately 15 hours and several autolysis peptides were observed.

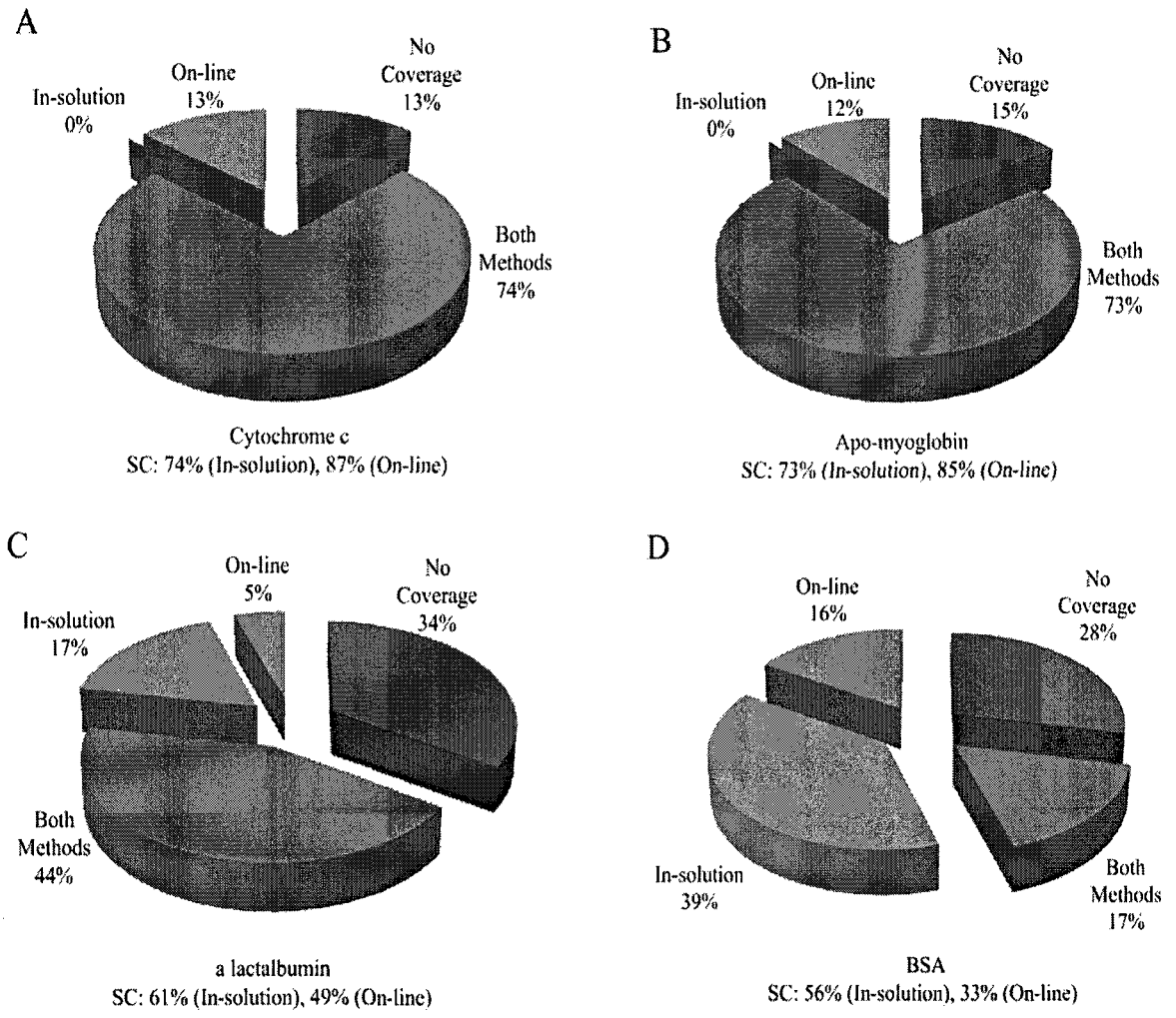

Figure 3-12: Pie chart representations for the digestion of four proteins comparing the sequence coverages for both in-solution and on-line with the digestor. For example in chart A cytochrome c was digested. Both methods had 74% of the sequence coverage in common but the on-line digestor had an additional 13% coverage producing a total of 87%. Both methods failed to produce peptides over 13% of the sequence (No Coverage); B) apo-myoglobin; C) α lactalbumin; D) BSA. SC: sequence coverage.

3.2.7 Summary of reactor characterization

Trypsin and Glu-C were immobilized onto the GMA grafted poly(BAC-co-BDDA-co-AMPS) monolith based capillary columns by taking advantage of a photografting technique. Elimination of protease autolysis means that it is not necessary

to use much more expensive sequencing grade proteases. The trypsin used in this thesis costs $0.0003/μg which is about 3000 times less than its sequencing grade counterpart at $0.9/μg. These reactors can be reused for a number of times and the digestion efficiency can be maintained for a long period of storage time.

The temperature and buffer pH studies suggested that the essential properties of trypsin and Glu-C were not altered by the immobilization process. The relatively high local concentration of the protease allowed model protein tryptic digestions to be completed within two minutes. This is in sharp contrast to the multiple hour in-solution digestions. The reactors' speed of digestion, comparable sequence coverages and lack of carry-over makes them potential candidates for on-line automated protein mixture analysis. By combining a fast separation step and an even faster enzymatic digestion step followed by MS detection, rapid on-line top-down proteomics may be feasible.

3.3 On-line enzyme reactor applications

3.3.1 On-line protein separation and tryptic digestion

The top-down approach in proteomics provides separated/purified proteins for digestion and subsequent identification steps. The peptide fragments of the target protein are produced through either chemical or enzymatic cleavages in order to generate sequence information and identification. The commonly used in-solution enzymatic digestion is inappropriate for an automated fluidic system for top-down analysis system. The two problems are the long incubation times (hours) and a substantial amount of sample handling. On the other hand, enzyme reactors containing immobilized proteases have the potential to overcome these bottlenecks. Based on the results obtained in Section 3.2, these reactors are capable of fast and high efficiency digestions of minute protein samples, while coupled to mass spectrometers. Given the versatility of the monolith and photografting strategy, two novel tandem columns were investigated.

3.3.1.1 Mobile phase composition

First, a protein separation coupled directly to a proteolytic digestor with on-line MS detection will be demonstrated. In this integrated flow-through system, the mobile phase containing both aqueous and organic solvents must be carefully balanced since it not only is the chromatographic mobile phase but it also provides buffer for protein digestion and must be compatible with MS detection (*i.e.* volatile and salt-free). Based on the success obtained from on-line protein digestion experiments, ammonium bicarbonate mixed with ACN was determined to be a suitable solvent. Moreover, in order to perform the on-line protein separation and digestion in tandem, the amount of ACN in the solvent needed to be a compromise between the high organic fractions that

provided adequate protein separation and the limited tolerance for organic solvents of the protease. Peterson *et al.* [101] have demonstrated enhanced stability of immobilized enzymes in dilute organic solvents which suggests that there may indeed be an advantage to having some organic content in the mobile phase.

One convenient method of assessing activity is to use a chromogenic substrate such as benzoyl-L-arginine 4-nitroanilide hydrochloride (BAPNA), but as has been discussed adsorption of BAPNA on the reactor' stationary phase prevented its use. Therefore, the BAPNA activity assay of trypsin was conducted in solution, and the assumption that the data should indicate a concentration of ACN that would not be detrimental to the immobilized enzymes in light of Peterson's findings, was made. Figure 3-13 shows that trypsin maintained its activity up to 20% ACN, but the activity rapidly decreased after 40% ACN and this correlates well with the wash experiments in Section 3.2.5. Therefore, a solvent system consisting of 50 mM ammonium bicarbonate, pH 8.0 and 20% ACN was used to perform an on-line isocratic protein separation followed by digestion.

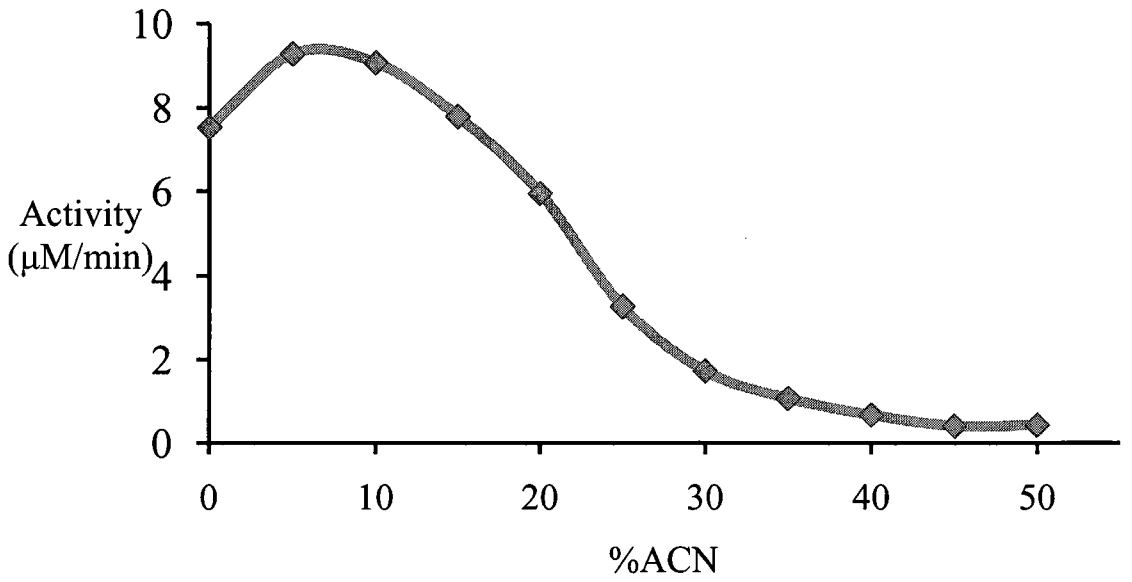

Figure 3-13: In-solution trypsin activity. The assay was conducted at 23 °C with 0.1 mg/mL trypsin in 50 mM ammonium bicarbonate, pH 8.0 in ACN with 2 mM BAPNA as a substrate.

3.3.1.2 Monolith surface modification by PEG

For on-line protein analysis, a relatively hydrophilic pore surface is desirable to minimize non-specific adsorption of protein and digestion products. This problem has been observed with methacrylate monoliths [110], including direct immobilization with the GMA functionality [67]. A popular approach to reduce protein/peptide adsorption is to modify the surface with hydrophilic polymers. In particular, neutral hydrophilic polymers, such as poly(ethylene glycol) (PEG), have been shown to be very effective [111], and is readily soluble in both water and many organic solvents. When coated on the monolith, PEG is thought to function by blocking of the adsorption sites for proteins and peptides [75]. Therefore, the potential for peptide adsorption on the monolith was investigated prior to the experiment of on-line protein separation and digestion by injecting a mixture of peptides (Table 3) with varying hydrophobicities [112] and charges

onto the monolithic columns that had varying amounts of trypsin (100% → 0%) and aminated PEG (0% → 100%) immobilized on the surface.

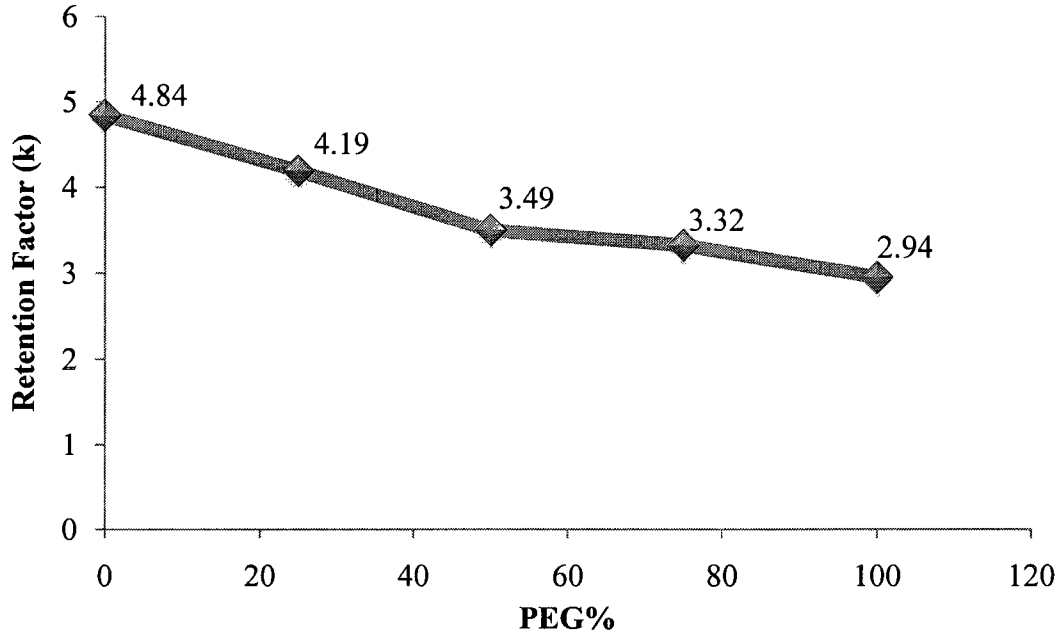

Figure 3-14: Retention factors of a peptide mixture in PEG modified trypsin reactors.

Interestingly, all peptides co-eluted (with 20% ACN) for all of the columns. The retention factor decreased steadily from 5 for a purely trypsin column through to 3 for a pure "PEG" column (Figure 3-14). This data suggests that there is some mode of retention at work but hydrophobic, size-exclusion or ion-exchange mechanisms would not explain the data since they would produce some selectivity amongst the peptides. At this time, there isn't an adequate explanation for the retention mechanism at work. These results do suggest that generated peptides will co-elute from the reactor and this is advantageous for proteomics since each protein peak would produce one mixed peptide peak in the MS rather than multiple peaks separated in time.

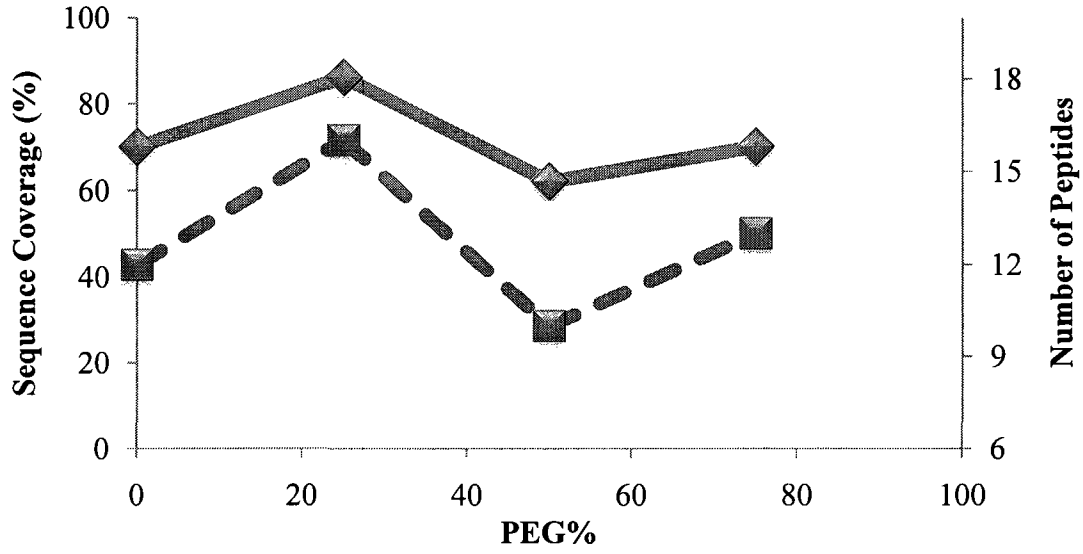

Figure 3-15: On-line cytochrome c digestions in PEG modified trypsin reactors. ♦ represents the cytochrome c sequence coverage from the digestion, and ■ represents the number of peptides detected.

With these same columns, cytochrome c digestions were performed. The sequence coverage was 72 ± 10 % (Figure 3-15) and did not show any systematic variation for the columns with trypsin. Hence, trypsin reactors without PEG modification were utilized for the subsequent experiments using on-line isocratic protein separation followed by digestion.

3.3.1.3 On-line tandem protein separation and digestion

Prior to conducting protein separation and digestion in tandem, separation of cytochrome c (83 pmol) and apo-myoglobin (55 pmol) was performed with the experimental set-up shown in Figure 2-6, but excluded the tryptic reactor connected after the monolithic separation column.

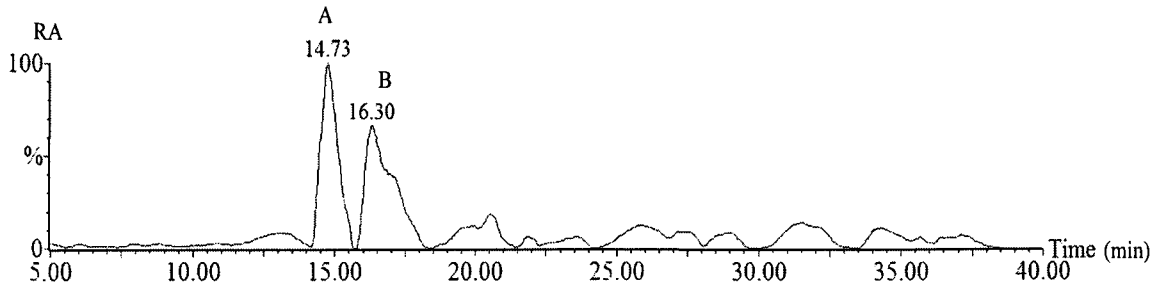

Figure 3-16: Total ion chromatogram of apo-myoglobin (A) and cytochrome c (B) separation. Isocratic conditions were applied using 20% ACN in 50 mM ammonium bicarbonate, pH 8.0 at 0.5 μL/min. The column eluate was diluted with 0.5 μL/min ACN and 0.1% formic acid. All MS conditions were the same as in Figure 3-6 except the cone voltage was 50 V. RA is the relative abundance of the ions.

The total ion chromatogram in Figure 3-16 showed that cytochrome c and apo-myoglobin are baseline separated on the base monolith. The difference in retention time between these two proteins was about 2 minutes, which should provide sufficient time for tryptic digestion downstream while maintaining the separation of the peptide products when they are eluted from the digestor. Since proteins are composed of a number of hydrophobic and charged amino acids which are either located on the surface exposed to the surrounding environment or embedded within the protein 3D structure, they can be separated according to the different degree of the interaction with the functional groups on the surface of the unmodified base monolith. Recall that the poly(BAC-co-BDDA-co-AMPS) monolith used in this experiment contains both C4 hydrophobic and sulfonate functionalities (AMPS). The results presented in Section 3.1.4 where five standard peptides were separated chromatographically suggest that a combination of hydrophobic and ionic interactions may be the mechanism responsible for the separation.

On-line protein separation *and digestion* using cytochrome c and apo-myoglobin was then carried out. The protein and peptide total ion current chromatogram and

corresponding MS spectra are presented in Figure 3-17 where eight peptides from apo-myoglobin were identified in the peak beginning at 18 minutes through to 20 minutes, yielding a sequence coverage of 44%. No peptides from cytochrome c were found in this region. Twenty peptides from cytochrome c were observed in the peak from 20 to 25 minutes and yielded a sequence coverage of 90% but there were two peptides from apo-myoglobin (*m/z* 992 and *m/z* 1076) that carried-over from the previous protein.

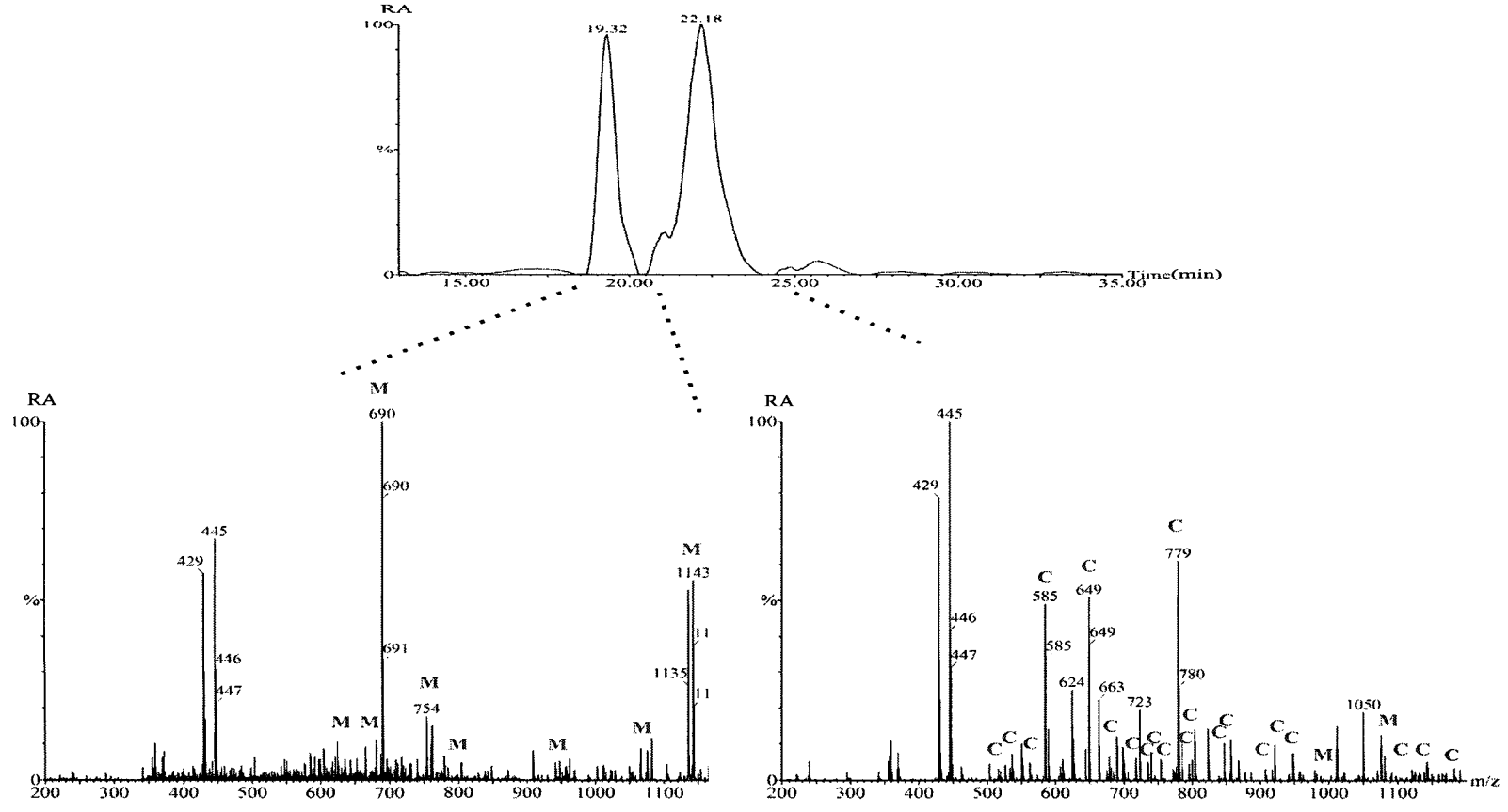

Figure 3-17: Total ion current chromatogram (top) and MS spectra (bottom) obtained from on-line cytochrome c and myoglobin separation followed by tryptic digestion. The MS spectrum (bottom left) corresponds to the peak from 18 – 20 min, and the MS spectrum (bottom right) represents the peaks from 20- 24 min in the chromatogram. Myoglobin and cytochrome c peptides are labelled with M and C, respectively. For MS analysis, the experimental conditions are given in Figure 3-6. RA is the relative abundance of the ions.

The data demonstrates that cytochrome c and apo-myoglobin were base-line separated by the monolithic column, and that the separation was maintained in the digestor even as the protein was degraded into peptides. It is noteworthy that the sequence coverage in this case was significantly lower for apo-myoglobin compared to the previous experiments where 85% was found. The explanation for the lower sequence coverage is that the mass of protein in this experiment was about one order of magnitude smaller than when the protein was (continuously) infused through the reactor and the missing peptides produced some of the lowest ion intensities relative to the peptides detected in both experiments. The possibility of loss of peptides in the reactor due to adsorption was discounted based on the coelution of injected peptides as explained in Section 3.3.1.2. The most important point of this experiment is that separation and identification of these two proteins via their peptides was completed within 30 min. With further efforts to improve the peak efficiency, for example by using these monoliths in CEC mode and increasing the mobile phase elutropic strength with additives, higher quality protein separations are possible [91]. Alternatively, a solid-phase extractor combined with an enzymatic microreactor [101] would be useful.

3.3.2 Digestion with dual enzyme reactor

A second type of tandem column was investigated where both trypsin and Glu-C were sequentially immobilized within one column by repeating the photografting and immobilization steps in separate areas of the column. Multiple, sequential, enzyme reactors have been known in the literature since the 1960's [113] and have recently been demonstrated in microfluidic devices [114], however, we believe that this is the first report of multiple proteolytic reactors being developed for proteomic applications.

ACTH, which has only one cleavage site for trypsin and one for Glu-C, was digested after each immobilization step. The digests were then analyzed by both CE and MS.

The CE separation of the ACTH and the digest is shown in Figure 3-18 where the two tryptic peptides were observed when only trypsin had been immobilized. After immobilization of Glu-C both the tryptic and Glu-C peptides were observed. The identity of these peptides was confirmed by MS analysis (data not shown). This simple example demonstrates that selective and sequential immobilization of enzymes through selective photografting is possible and allows the reactor to be tailored to specific applications. For example, the length of each reactor zone can be easily adjusted to yield the optimal contact time for a given flow rate. Other combinations are also easily achieved such as deglycosylation enzymes (PNGase F) followed by proteolytic digestion to simplify glycoprotein analysis.

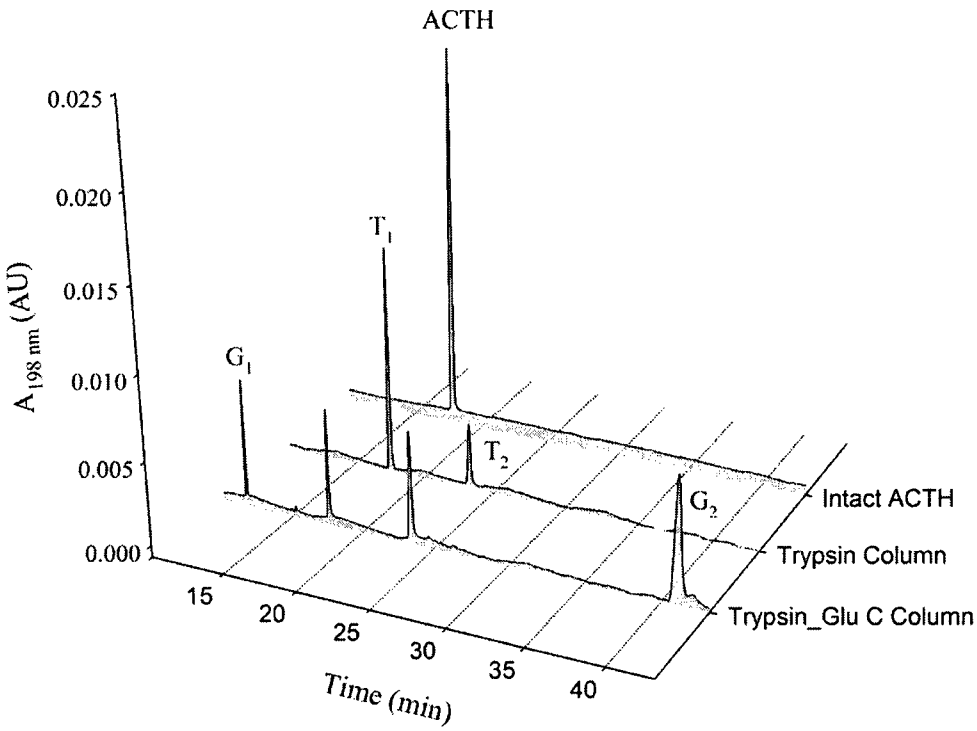

Figure 3-18: CE separation of ACTH and digest. From top, 1) Intact ACTH; 2) ACTH digested by trypsin reactor; 3) ACTH digested by trypsin+Glu C reactor. A separation voltage of 15 kV was applied to the 60 cm (50 cm to window) 75 μm ID capillary with 50 mM phosphate, pH 2.5 as BGE. Samples were injected using a 5 second, 34.5 mbar hydrodynamic injection and separated at 28 °C. T1 and T2 are tryptic peptides; G1 and G2 are Glu-C peptides.

Conclusions and Future work

Monolithic supports are suitable substrates for synthesis of high performance analytical devices. With site-specific UV photografting, monoliths can be tailored to accommodate multiple functionalities including single or multiple enzyme reactors. Throughout this thesis, polymer-based monolithic tryptic and Glu-C reactors have been fabricated in fused-silica capillaries, and characterized through protein digestion and identification by MALDI and ESI-MS. An approach to immobilize both trypsin and Glu-C onto a dual-functional enzyme reactor has also been demonstrated. Importantly, high digestion efficiency was obtained with short contact times. Furthermore, a monolithic separation and tryptic reactor showed that protein separation and digestion can be integrated. With further development, high throughput separations and digestion of a protein mixture is possible for "top-down" proteomics applications. To accomplish this will require coming to a better understanding, and reduction, of peptide retention in the digestor and increasing the protein separation efficiency, possibly by exploiting electro driven flow using the residual AMPS functionalities.

For the future work, there are several aspects which should be investigated further. There is no universal column that can be used to analyze both large molecules and small molecules. Small molecules and peptides require columns with the average pore sizes between 6 and 35 nm, whereas large biomolecules need pore sizes from 50 to 400 nm. Therefore, the balance of macropores and micropores within the columns should be adjusted to favour a specific task. The experimental conditions to produce a monolith, *e.g.* composition of the porogenic solvent and temperature, should be systematically studied in order to produce tailored monolithic columns with defined pore sizes.

Moreover, the separation mechanism using the poly(BAC-BDDA-AMPS) should be explored in order to perform separations on complex samples. More controlled experiments are needed to understand the degree of contribution from AMPS during chromatographic separations.

A continuing problem is the need for an easy proteolytic assay, so a new method should be investigated to assay activity of the immobilized proteases. A new substrate is required to facilitate sensitive detection while having no adsorption to the monolithic backbone.

Another experiment that is worth further exploring is determining an effective and shorter inter-digestion wash method so that overall system efficiency/throughput can be improved.

Finally, as the adage says "the proof of the pudding is in the tasting" so testing the digestor with complex samples or real biological samples, especially using the dual-functional enzyme reactors needs to be explored and evaluated.

References

[1] Twyman, R. M., *Principles of Proteomics*, Garland Science/BIOS Scientific Publishers, New York, NY 2004.

[2] Stenesh, J., *Dictionary of Biochemistry*, Wiley-Interscience, New York, NY 1983.

[3] Gomase, V. S., Kale, K. V., Tagore, S., Hatture, S. R., *Current drug metabolism* 2008, *9(3)*, 213-220.

[4] Sleno, L., Emili, A., *Current Opinion in Chemical Biology* 2008, *12*, 46-54.

[5] Wasinger, V. C., Cordwell, S. J., Cerpa-Poljak, A., Yan, J. X., Gooley, A. A., Wilkins, M. R., Duncan, M. W., Harris, R., Williams, K. L., Humphery-Smith, I., *Electrophoresis* 1995, *16*, 1090-1094.

[6] Lundblad, R. L., *The Evolotion from Protein Chemistry to Proteomics*, CRC Press, Boca Raton, FL 2006.

[7] Kelleher, N. L., *Anal. Chem.* 2004, *76*, 196A-203A.

[8] Han, X., Aslanian, A., Yates III, J. R., *Current Opinion in Chemical Biology* 2008, *12*, 483-490.

[9] Allen, G., *Sequencing of Proteins and Peptides*, Elsevier, Amsterdam 1989.

[10] Washburn, M. P., Wolters, D., Yates, J. R., *Nat. Biotech* 2001, *19*, 242-247.

[11] Švec, F., *Electrophoresis* 2006, *27*, 947-961.

[12] Massolini, G., Calleri, E., *J. Sep. Sci.* 2005, *28*, 7-21.

[13] Ma, J., Zhang, L., Liang, Z., Zhang, W., Zhang, Y., *J. Sep. Sci.* 2007, *30*, 3050-3059.

[14] Křenková, J., Foret, F., *Electrophoresis* 2004, *25*, 3550-3563.

[15] Calleri, E., Temporini, C., Perani, E., Stella, C., Rudaz, S., Lubda, D., Mellerio, G., Veuthey, J. L., Caccialanza, G., Massolini, G., *J. Chromatogr. A* 2004, *1045*, 99-109.

[16] Palm, A. K., Novotny, M. V., *Rapid Commun. Mass Spectrom.* 2004, *18*, 1374-1382.

[17] Turková J, Bláha K, Malaníková M, Vancurová D, Švec F, Kálal J, *Biochim. Biophys. Acta* 1978, *524*, 162-165.

[18] Benčina, K., Podgornik, A., Štrancer, A., Benčina, M., *J. Sep. Sci.* 2004, *27*, 811-818.

[19] Hearn, W., Bethell, G. S., Ayers, J. S., Hancock, W. S., *J. Chromatogr.* 1979, *185*, 463-470.

[20] Temporini, C., Calleri, E., Campèse, D., Cabrera, K., Félix, G., Massolini, G., *J. Sep. Sci.* 2007, *30*, 3069-3076.

[21] Kato, M., Sakai-Kato, K., Jin, H. M., Kubota, K., Miyano, H., Toyo'oka, T., Dulay, M. T., Zare, R. N., *Anal. Chem.* 2004, *76*, 1896-1902.

[22] Stigter, E. C. A., de Jong, G. J., van Bennekom, W. P., *Anal. Chim. Acta* 2008, *619*, 231-238.

[23] Lim, Y.-P., Josic, D., Callanan, H., Brown, J., Hixson, D. C., *J. Chromatogr. A* 2005, *1065*, 39-43.

[24] Luo, Q., Mao, X., Kong, L., Huang, X., Zou, H., *J. Chromatogr. B* 2002, *776*, 139-147.

[25] Calleri, E., Marrubini, G., Massolini, G., Lubda, D., de Fazio, S. S., Furlanetto, S., Wainer, I. W., Manzo, L., Caccialanza, G., *J. Pharm. Biomed. Anal.* 2004, *35*, 1179-1189.

[26] Gao, J., Xu, J., Locascio, L. E., Lee, C. S., *Anal. Chem.* 2001, *73*, 2648-2655.

[27] Cooper, J. W., Chen, J., Li, Y., Lee, C. S., *Anal. Chem.* 2003, *75*, 1067-1074.

[28] Amankwa, L. N., Kuhr, W. G., *Anal. Chem.* 1993, *65*, 2693-2697.

[29] Turková, J., *J. Chromatogr. B* 1999, *722*, 11-31.

[30] Sakai-Kato, K., Kato, M., Toyo'oka, T., *Anal. Chem.* 2002, *74*, 2943-2949.

[31] Sakai-Kato, K., Kato, M., Toyo'oka, T., *Anal. Chem.* 2003, *75*, 388-393.

[32] Nouaimi, M., Möschel, K., Bisswanger, H., *Enzyme Microb. Technol.* 2001, *29*, 567-574.

[33] Yao, T., Nanjyo, Y., *BUNSEKIKAGAKU* 2001, *50*, 603-611.

[34] Amankwa, L. N., Kuhr, W. G., *Anal. Chem.* 1992, *64*, 1610-1613.

[35] Liu, Y., Xue, Y., Ji, J., Chen, X., Kong, J., Yang, P., Girault, H. H., Liu, B., *Mol. Cell. Proteomics* 2007, *6*, 1428-1436.

[36] Liu, Y., Qu, H., Xue, Y., Wu, Z., Yang, P., Liu, B., *Proteomics* 2007, *7*, 1373-1378.

[37] Urban, J., Jandera, P., *J. Sep. Sci.* 2008, *31*, 2521-2540.

[38] Hjertén, S., Liao, J. L., Zhang, R., *J. Chromatogr.* 1989, *473*, 273-275.

[39] Tennikova, T. B., Belenkii, B. G., Švec, F., *J. Liq. Chromatogr.* 1990, *13*, 63-70.

[40] Švec, F., Fréchet, J. M. J., *Anal. Chem.* 1992, *64*, 820-822.

[41] Svec, F., *Recent Developments in LC Column Technology* 2003.

[42] Calleri, E., Massolini, G., Lubda, D., Temporini, C., Loiodice, F., Caccialanza, G., *J. Chromatogr.* 2004, *1031*, 93-100.

[43] Kato, M., Inuzuka, K., Sakai-Kato, K., Toyo'oka, T., *Anal. Chem.* 2005, *77*, 1813-1818.

[44] Dulay, M. T., Baca, Q. J., Zare, R. N., *Anal. Chem.* 2005, *77*, 4604-4610.

[45] Gaber A. M. Mersal, U. B., *Electrophoresis* 2005, pp. 2303-2312.

[46] Palm, A. K., Novotny, M. V., *Rapid Commun. Mass Spectrom.* 2005, *19*, 1730-1738.

[47] Vodopivec, M., Podgornik, A., Berovič, M., Štrancar, A., *J. Chromatogr. B* 2003, *795*, 105-113.

[48] Coleman, P. L., Walker, M. M., Milbrath, D. S., Stauffer, D. M., *J. Chromatogr. A* 1990, *512*, 345-363.

[49] Drtina, G. J., Haddad, L. C., Rasmussen, J. K., Gaddam, B. N., Williams, M. G., Moeller, S. J., Fitzsimons, R. T., Fansler, D. D., Buhl, T. L., Yang, Y. N., Weller, V. A., Lee, J. M., Beauchamp, T. J., Heilmann, S. M., *Reactive and Functional Polymers* 2005, *64*, 13-24.

[50] Xie, S., Svec, F., Fréchet, J. M. J., *Biotech. Bioeng.* 1999, *62*, 30-35.

[51] Peterson, D. S., Rohr, T., Švec, F., Fréchet, J. M. J., *Anal. Chem.* 2002, *74*, 4081-4088.

[52] Vlakh, E. G., Tennikova, T. B., *J. Sep. Sci.* 2007, *30*, 2801-2813.

[53] Cabrera, K., *J. Sep. Sci.* 2004, *27*, 843-852.

[54] Snyder, L., Kirkland, J., *Introduction to Modern Liquid Chromatography*, Wiley, New York 1979.

[55] Wiseman, A.,*Handbook of enzyme biotechnology*, Horwood 1985, pp. 54-142.

[56] Yang, Y., Velayudhan, A., Ladisch, C. M., Ladisch, M. R., *J. Chromatogr. A* 1992, *598*, 169-180.

[57] Petro, M., Švec, F., Fréhet, J. M. J., *Biotechnol. Bioeng.* 1996, *49*, 355-363.

[58] Švec, F., Fréchet, J. M. J., *Macromolecules* 1995, *28*, 7580-7582.

[59] Viklund, C., Švec, F., Fréchet, J. M. J., Irgum, K., *Chem. Mater.* 1996, *8*, 744-750.

[60] Tennikova, T. B., Svec, F., *J. Chromatogr. A* 1993, *646*, 279-288.

[61] Ueki, Y., Umemura, T., Iwashita, Y., Odake, T., Haraguchi, H., Tsunoda, K.-i., *J. Chromatogr. A* 2006, *1106*, 106-111.

[62] Švec, F., Fréhet, J. M. J., *Biotechnol. Bioeng.* 1995, *48*, 476-480.

[63] Kasper, C., Meringova, L., Freitag, R., Tennikova, T., *J. Chromatogr. A* 1998, *798*, 65-72.

[64] Potter, O. G., Breadmore, M. C., Hilder, E. F., *Analyst* 2006, 1094 - 1096.

[65] Benčina, M., Benčina, K., Štrancar, A., Podgornik, A., *J. Chromatogr. A* 2005, *1065*, 83-91.

[66] Bartolini, M., Cavrini, V., Andrisano, V., *J. Chromatogr. A* 2005, *1065*, 135-144.

[67] Křenková, J., Bilková, Z., Foret, F., *J. Sep. Sci.* 2005, *28*, 1675-1684.

[68] Valentová, O., Marek, M., Švec, F., Štamberg, J., Vodrážka, Z., *Biotechnol. Bioeng.* 1981, *23*, 2093-2104.

[69] Rohovec, J., Maschmeyer, T., Aime, S., Peters, J. A., *Chemistry - A European Journal* 2003, *9*, 2193-2199.

[70] Rånby, B., Yang, W. T., Tretinnikov, O., *Nucl. Instrum. Methods Phys. Res., Sect. B* 1999, *151*, 301-305.

[71] Rohr, T., Hilder, E. F., Donovan, J. J., Švec, F., Fréchet, J. M. J., *Macromolecules* 2003, *36*, 1677-1684.

[72] Kienková, J., Foret, F., *Electrophoresis* 2004, *25*, 3550-3563.

[73] VandeVondele, S., Vörös, J., Hubbell, J. A., *Biotechnol. Bioeng.* 2003, *82*, 784-790.

[74] Gombotz, W. R., Guanghui, W., Horbett, T. A., Hoffman, A. S., *Journal of Biomedical Materials Research* 1991, *25*, 1547-1562.

[75] McPherson, T., Kidane, A., Szleifer, I., Park, K., *Langmuir* 1998, *14*, 176-186.

[76] Ye, M., Hu, S., Schoenherr, R. M., Dovichi, N. J., *Electrophoresis* 2004, *25*, 1319-1326.

[77] Ivanov, A. R., Zang, L., Karger, B. L., *Anal. Chem.* 2003, *75*, 5306-5316.

[78] Samskog, J., Bylund, D., Jacobsson, S. P., Markides, K. E., *J. Chromatogr. A* 2003, *998*, 83-91.

[79] Li, Y., Cooper, J. W., Lee, C. S., *J. Chromatogr. A* 2002, *979*, 241-247.

[80] Geiser, L., Eeltink, S., Švec, F., Fréchet, J. M. J., *J. Chromatogr. A* 2008, *1188*, 88-96.

[81] Temporini, C., Dolcini, L., Abee, A., Calleri, E., Galliano, M., Caccialanza, G., Massolini, G., *J. Chromatogr. A* 2008, *1183*, 65-75.

[82] Křenková, J., Kleparnik, K., Foret, F., *J. Chromatogr. A* 2007, *1159*, 110-118.

[83] Licklider, L., Kuhr, W. G., Lacey, M. P., Keough, T., Purdon, M. P., Takigiku, R., *Anal. Chem.* 1995, *67*, 4170-4177.

[84] Drapeau, G. R., Laszlo, L.,*Protease from Staphyloccus aureus*, Academic Press, New York 1976, pp. 469-475.

[85] Ngola, S. M., Fintschenko, Y., Choi, W. Y., Shepodd, T. J., *Anal. Chem.* 2001, *73*, 849-856.

[86] Hilder, E. F., Švec, F., Fréchet, J. M. J., *Anal. Chem.* 2004, *76*, 3887-3892.

[87] Brunauer, S., Emmett, P. H., Teller, E., *J. Am. Chem. Soc.* 1938, *60*, 309-319.

[88] Progent, F., Augustin, V., Tran, N. T., Descroix, S., Taverna, M., *Electrophoresis* 2006, *27*, 757-767.

[89] Karas, M., Hillenkamp, F., *Anal. Chem.* 1988, *60*, 2301 - 2303.

[90] Eeltink, S., Geiser, L., Švec, F., Fréchet, J. M. J., *J. Sep. Sci.* 2007, *30*, 2814-2820.

[91] Bandilla, D., Skinner, C. D., *J. Chromatogr. A* 2003, *1004*, 167-179.

[92] Cabral, J.-L.,*Development of a New Strategy for the Modification of Monolithic Stationary Phases used in Capillary Electrochromatography*, Concordia University, Montreal 2007, p. 216.

[93] Cabral, J. L., Bandilla, D., Skinner, C. D., *J. Chromatogr. A* 2006, *1108*, 83-89.

[94] Eeltink, S., Hilder, E. F., Geiser, L., Švec, F., Fréchet, J. M. J., Rozing, G. P., Schoenmakers, P. J., Kok, W. T., *J. Sep. Sci.* 2007, *30*, 407-413.

[95] Leofanti, G., Padovan, M., Tozzola, G., Venturelli, B., *Catal. Today* 1998, *41*, 207-219.

[96] Gooding, K. M., Regnier, F. E.,*HPLC of Biological Macromolecules*, CRC Press, Boca Raton 2002, pp. 81-247.

[97] Hilder, E. F., Švec, F., Fréchet, J. M. J., *Electrophoresis* 2002, *23*, 3934-3953.

[98] Delaunay-Bertoncini, N., Demesmay, C., Rocca, J.-L., *Electrophoresis* 2004, *25*, 3204-3215.

[99] Migneault, I., Dartiguenave, C., Vinh, J., Bertrand, M. J., Waldron, K. C., *Electrophoresis* 2004, *25*, 1367-1378.

[100] Temporini, C., Perani, E., Mancini, F., Bartolini, M., Calleri, E., Lubda, D., Felix, G., Andrisano, V., Massolini, G., *J. Chromatogr. A* 2006, *1120*, 121-131.

[101] Peterson, D. S., Rohr, T., Švec, F., Fréchet, J. M. J., *Anal. Chem.* 2003, *75*, 5328-5335.

[102] Chalfie, M., Tu, Y., Euskirchen, G., Ward, W. W., Prasher, D. C., *Science* 1994, *263*, 802-805.

[103] Buck, F. F., Vithayathil, A. J., Bier, M., Nord, F. F., *Arch. Biochem. Biophys.* 1962, *97*, 417-424.

[104] Ding, L., Li, Y., Jiang, Y., Cao, Z., Huang, J., *J. Appl. Polym. Sci.* 2002, *83*, 94-102.

[105] Huang, X. L., Catignani, G. L., Swaisgood, H. E., *J. Biotechnol.* 1997, *53*, 21-27.

[106] Koskinen, A., Kilbanov, A. M., *Enzymatic reactions in organic media*, Springer, London 1996.

[107] Mozhaev, V. V., Martinek, K., *Eur. J. Biochem.* 1981, *115*, 143.

[108] Al-Lawati, H., Watts, P., Welham, K. J., *Analyst* 2006, 656 - 663.

[109] Křenková, J., Lacher, N. A., Švec, F., *Anal. Chem.* 2009, *81*, 2004-2012.

[110] Stachowiak, T. B., Švec, F., Fréchet, J. M. J., *Chem. Mater.* 2006, *18*, 5950-5957.

[111] Harris, J. M.,*Introduction to biotechnical and biomedical applications of poly(ethylene glycol)*, Plenum Press, New York 1992.

[112] Hopp, T. P., Woods, K. R., *Proc. Natl. Acad. Sci. U. S. A.* 1981, *78(6)*, 3824 - 3828.

[113] Brown, H. D., Patel, A. B., Chattopadhyay, S. K., *J. Chromatogr.* 1968, *35*, 103-105.

[114] Logan, T. C., Clark, D. S., Stachowiak, T. B., Švec, F., Fréchet, J. M. J., *Anal. Chem.* 2007, *79*, 6592-6598.

Appendix A: Brunauer-Emmett-Teller Equation

$$V_{ads} = V_m \frac{cp/p_s}{1-p\not{p}_s} \frac{1-(n+1)(p\not{p}_s)^n + n(p\not{p}_s)^{n+1}}{1+(c-1)(p\not{p}_s)^n + c(p\not{p}_s)^{n+1}}$$

Equation A_1: V_{ads} and V_m are the adsorbed volume and the monolayer volume, respectively. c is related to heat of adsorption and liquefaction, and n is related to the mean number of layer that can be formed on the solid. p/p_s is relative pressure.

If $n \rightarrow \infty$, Equation assumes the following form:

$$V_{ads} = V_m \frac{cp/p_s}{(1-p\not{p}_s)(1+(c-1)\,p\not{p}_s}$$

Equation A_2: This equation is suitable for $n > 6$.

Appendix B: Taverna's Method for Electrokinetic Total Porosity

Equation for total porosity:

$$\varepsilon_T = \frac{L_e \emptyset}{L_{pack}}$$

Equation B_1: ε_T represents total porosity. L_{pack} and L_e are, respectively, the packed length of the capillary column and the effective length of the flow path. $\emptyset$ represents the conductivity ratio of the packed segment and of the open capillary column.

L_e can be evaluated by the following equation:

$$L_e = L_{tot} \sqrt{\frac{I_{open}}{I_{pack}}} - L_{open}$$

Equation B_2: L_{tot} is the total length of the capillary column, and L_{open} is the length of the open segment of the packed column. I_{open} and I_{pack} are the current intensities measured through an open capillary column and the packed column, respectively.

$\emptyset$ can be assessed by the following equation:

$$\emptyset = \frac{\frac{L_{pack}}{L_{tot}}}{\frac{I_{open}}{I_{pack}} - (1 - \frac{L_{pack}}{L_{tot}})}$$

Equation B3: Conductivity ratio between the packed segment of the packed capillary column and the open column.

Appendix C: Protein Sequence

Cytochrome c

Total Length: 105 Amino Acids

MW: 11,832 Da

MGDVEKGKKIFVQKCAQCHTVEKGGKHKTGPNLHGLFGRKTGQAPGFTYTDA
NKNKGITWKEETLMEYLENPKKYIPGTKMIFAGIKKKTEREDLIAYLKKATNE

Apo-myoglobin

Total Length: 154 Amino Acids

MW: 17,072 Da

MGLSDGEWQQVLNVWGKVEADIAGHGQEVLIRLFTGHPETLEKFDKFKHLKTE
AEMKASEDLKKHGTVVLTALGGILKKKGHHEAELKPLAQSHATKHKIPIKYLEFI
SDAIIHVLHSKHPGDFGADAQGAMTKALELFRNDIAAKYKELGFQG

α lactalbumin

Total Length: 123 Amino Acids

MW: 14,175 Da

EQLTKCEVFRELKDLKGYGGVSLPEWVCTAFHTSGYDTQAIVQNNDSTEYGLFQ
INNKIWCKDDQNPHSSNICNISCDKFLDDDLTDDIMCVKKILDKVGINYWLAHKA
LCSEKLDQWLCEKL

Bovine Serum Albumin

Total Length: 607 Amino Acids

MW: 69,293 Da

MKWVTFISLLLLFSSAYSRGVFRRDTHKSEIAHRFKDLGEEHFKGLVLIAFSQYL
QQCPFDEHVKLVNELTEFAKTCVADESHAGCEKSLHTLFGDELCKVASLRETYG
DMADCCEKQEPERNECFLSHKDDSPDLPKLKPDPNTLCDEFKADEKKFWGKYL
YEIARRHPYFYAPELLYYANKYNGVFQECCQAEDKGACLLPKIETMREKVLASS

ARQRLRCASIQKFGERALKAWSVARLSQKFPKAEFVEVTKLVTDLTKVHKECCH
GDLLECADDRADLAKYICDNQDTISSKLKECCDKPLLEKSHCIAEVEKDAIPENLP
PLTADFAEDKDVCKNYQEAKDAFLGSFLYEYSRRHPEYAVSVLLRLAKEYEATL
EECCAKDDPHACYSTVFDKLKHLVDEPQNLIKQNCDQFEKLGEYGFQNALIVRY
TRKVPQVSTPTLVEVSRSLGKVGTRCCTKPESERMPCTEDYLSLILNRLCVLHEK
TPVSEKVTKCCTESLVNRRPCFSALTPDETYVPKAFDEKLFTFHADICTLPDTEKQ
IKKQTALVELLKHKPKATEEQLKTVMENFVAFVDKCCAADDKEACFAVEGPKL
VVSTQTALA

Adrenocorticotropic Hormone Fragment 1-10 Human

Total Length: 10 Amino Acids

MW: 1,299 Da

SYSMEHFRWG

Appendix D: Theoretical Peptide Masses of Cytochrome c

The theoretical peptide masses of cytochrome c were generated using the program "PeptideMass" from the ExPASy World Wide Web server, at the URL address: http://www.expasy.ch/www/tools.html.

Table 7: The theoretical peptide masses of cytochrome c from trypsin digestions.

Mass	MC	Peptide Sequence
1495.70	0	EETLMEYLENPK
1470.69	0	TGQAPGFTYTDANK
1168.62	0	TGPNLHGLFGR
1018.44	0	CAQCHTVEK
964.53	0	EDLIAYLK
779.45	0	MIFAGIK
678.38	0	YIPGTK
678.31	0	MGDVEK
634.39	0	IFVQK
604.35	0	GITWK
434.19	0	ATNE
405.21	0	TER
284.17	0	HK
261.16	0	NK
261.16	0	GGK
204.13	0	GK
147.11	0	K

*MC is the number of missed cleavages.

Table 8: The theoretical peptide masses of cytochrome c from Glu-C digestions.

Mass	MC	Peptide Sequence
4469.32	0	KGGKHKTGPNLHGLFGRKTGQAPGFTYTDANKNKGITWKEE
2392.38	0	NPKKYIPGTKMIFAGIKKKTE
1947.03	0	KGKKIFVQKCAQCHTVE
1378.76	0	DLIAYLKKATNE
550.22	0	MGDVE
493.23	0	TLME
424.21	0	YLE
304.16	0	RE

*MC is the number of missed cleavages.